Carbon Based Nanocomposite Films for Packaging Applications

By

Misbah Iqbal

School of Chemical and Materials Engineering

National University of Sciences and Technology

2020

Carbon Based Nanocomposite Films for Packaging Applications

Name: Misbah Iqbal

Reg. No.: 00000205398

This work is submitted as a MS thesis in partial fulfillment of the requirement for the degree of

MS in Chemical Engineering

Supervisor Name: Dr. M. Bilal Khan Niazi

School of Chemical and Materials Engineering (SCME)

National University of Sciences and Technology (NUST)

H-12 Islamabad, Pakistan

August, 2020

Dedication

This thesis is dedicated to my beloved parents, dearest husband, siblings and in-laws.

This would not have been possible without their myriad love, support and encouragement.

Acknowledgements

Alhamdulillah, all praise to **Allah Almighty** whose worth cannot be described in words, whose blessings cannot be counted, all thanks to Him for giving me strength and courage to complete my research.

I am extremely obliged to my research supervisor **Dr. M. Bilal Khan Niazi** for his continuous support, impressive guidance and remarkable suggestions throughout the research work.

I am thankful to my evaluation committee members **Dr. Zaib Jahan** and **Dr. Zakir Hussain** for their valued suggestions and guidance.

I am grateful to **Dr. Tayyaba Noor** and **Dr. Sofia Javed** for allowing me to work in their respective labs.

I am also thankful to **Dr. Erum Pervaiz** for helping me in my research work.

I must express my deepest appreciation to my beloved parents and siblings who encouraged me to fullfill my dream of doing masters in chemical engineering and got me admitted in SCME NUST. I am also indebted to my dearest husband **Abdul Basit** and in-laws who fully cooperated in my studies and motivated me to pursue the research with full enthusiasm.

In the end, I am also thankful to my friends **Tasmia Azam**, **Amber Salim,** and **Aniza Nasir** who were always there for me.

Misbah Iqbal

Abstract

Plastic poses great hazard to our environment because of its non biodegradability as well as limited disposal methods. Ecofriendly biodegradable packaging is an excellent alternative to this. Biodegrable films based on PVA, starch and containing graphene oxide, in-situ and ex-situ reduced graphene oxide were sucessfully synthesized and tested for food packaging application. PVA and starch membrane having 0.4% wt/wt of in situ reduced graphene (PVA/St/IrGO20) showed exceptional mechanical properties i.e. tensile strength of 22.719 MPa and outstanding antibacterial activity exhibiting 38.89±0.23mm and 37.52±0.41mm zone of inhbition against Escherichia Coli and Staphylococcus Aureus respectively. PVA/starch membrane containg 0.2% wt/wt of ex situ reduced graphene oxide (PVA/St/XrGO10) showed comparable results. Surface morphology of the membranes confirmed that they were dense having no obvious pores. The synthesized membranes degraded almost completely after being buried in soil for just a single day. Among all the synthesized membranes, PVA/St/IrGO20 and PVA/St/XrGO10 prolonged the shelf life of packed Phyllanthus emblica since they acted as an excellent water vapor and gas barrier. After a number of tests, it was concluded that PVA/St/IrGO20 membranes showed remarkable antibacterial, thermal and barrier properties.

Table of Contents

List of Figures

List of Tables

Chapter 1

Introduction

1.1 Importance of food packaging:

Food is the basic necessity of life. Its importance for the mankind is unquestionable. Food packaging is the method applied in food industry to preserve food quality, retain its flavor and enhance the shelf life [1, 2]. This also maintains safety during transport and prevents food from the influence of external factors [3] like odor, dust, temperature, humidity, microorganisms etc. Packaging works as a natural shield to save food against external variables [1]. Stability of packaging materials is essential for improving food quality and safety. Packaging materials can fulfill their role in offering attractive, cost-effective, robust and convenient goods to consumers.

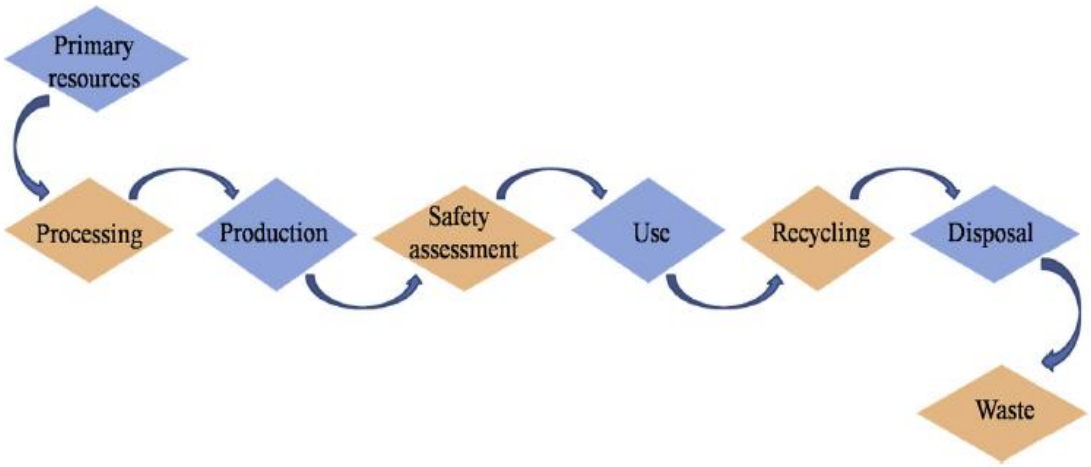

Figure 1 Complete life cycle of food packaging material [4]

The demand for healthy and fresh food, particularly fruits and vegetables, has gradually increased over the past decade in a context where eating and consumption habits have constantly changed owing to the lifestyle of society. For this reason, the European Union has created fresh goals for the food packaging sector: sustainability of raw materials, waste minimization and decrease of energy consumption.

1.2 Plastic Pollution an Environmental Concern:

The utilization of plastic appears to be appealing owing to its viable design, low price and lighter weight [5]. However, these materials are petroleum-based derivatives that are of noteworthy concern with regard to the disposal of waste [6, 7]. As per a recent study around 8 million tons of plastic are deliberately thrown away into oceans that find their way through water channels thereby destroying the aquatic life and causing water pollution. It is appalling to know that a simplest shopping bag, that is made of a very meek plastic, takes more than 100 years to collapse while this period is between 100 to 600 years or even more in case of complex ones.

It is expected that food wrappings and containers cause 31.15% pollution in the environment while containers and bottles' caps cause 15.5%. Environmental pollution due to plastic bags is 11.18%, beverage bottles cause 7.27% and 8.13% resulting from straw and stirrers. Plastic pollution has negative effects because it disrupts the food chain, contaminates ground water, soil and air.

On World Environment Day every year, there is a specific theme which major corporations, communities, non-governmental organizations, governments and celebrities worldwide adopt to promote environmental awareness. On occasion of World Environment Day on 5 June 2018, Sindh Environmental Protection Agency (SEPA) arranged a round table conference in alliance with the National Forum for Environment and Health (NFEH) and other stake holders with the theme "Beat Plastic Pollution".

1.3 Waste Management Approach:

Food industry is the first consumer of packaging materials [2]. Therefore, a slight decrease in materials used for packaging would lead to momentous cost reduction and a perfect solution of handling waste.

The most encouraging option of waste management is the reduction in source. However, waste diposal is the least favorable option. The benefits of the conventional packaging materials can not hinder and diminish the disadvantages. Diverse sum research has been conducted to counterbalance environmental safety and conservation demands with a main focus on packaging materials that can degrade in soil [8]. Keeping in record the above

mentioned facts, it is an alarming situation that demands the alternates of plastic packaging. One of which is biodegradable packaging.

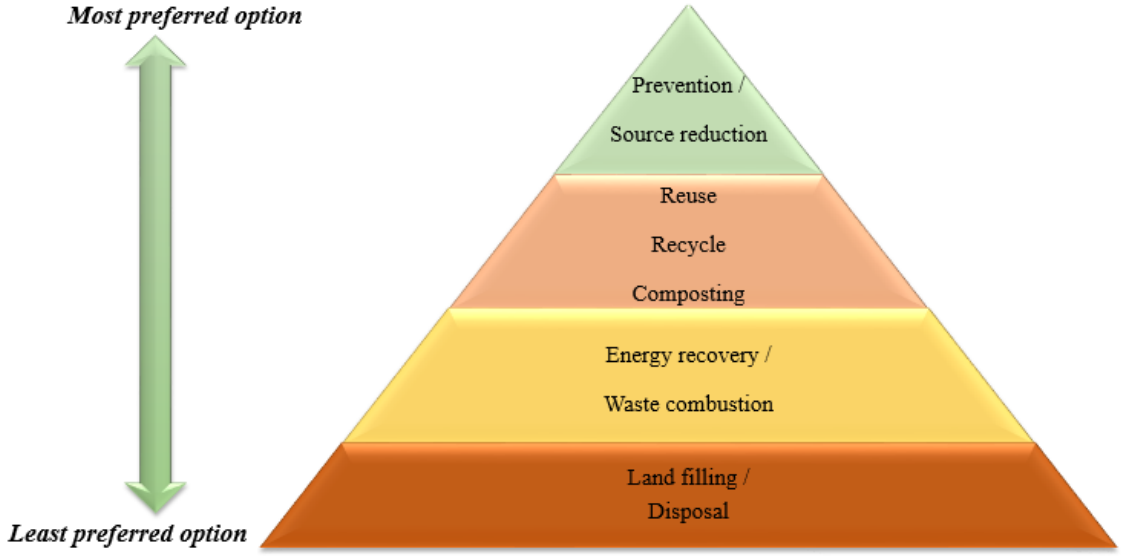

Figure 2 Waste Management Approach [9]

1.4 Driving force of Food Packaging Innovations:

The food packaging industry is driven generally to fulfill the socio-economic needs. Thus the packaging innovations must be accomplished by conveying high caliber and safe nourishment items to the customer in a productive way. Some of the socioeconomic needs that drive the innovations in food packaging are listed below [10]:

1.4.1 Improved Lifestyle:

Due to improvement in consumer lifestyle, there is a constant need of innovative food packaging that meets their needs and is accessible, tasteful, affordable, healthy and full of nutrition. The busy routine of individual makes it difficult to cook the time consuming dishes. So, they prefer microwavable or precooked meal, canned or refrigerated meal as well as the ready to go snacks.

1.4.2 Enhanced Value:

Value is the ratio of benefits to cost calculated by consumer. Thus value can be added either by reducing cost or increasing the benefits. Benefits can be enhanced by improving the functions of the package, to fulfill the extra needs of customers. Cost can be reduced

by utilizing economical packaging material, utilizing machines to save time and pack more items in less time. However, one must keep in mind that reducing the cost of package must not sacrifice the quality and safety of product.

1.4.3 Food Safety:

According to an estimate by Center for Disease Control and Prevention (CDCP), foodborne diseases lead to almost 128000 hospitalizations, 48 million illnesses and around 3000 deaths. Thus there is a greater need of enhanced food safety from microbial contamination which is the main cause of foodborne diseases. Microbial contamination may develop during harvesting, storage, handling, delivery, display, and preparation of food. Food can be protected from microbial contamination by using antibacterial packaging.

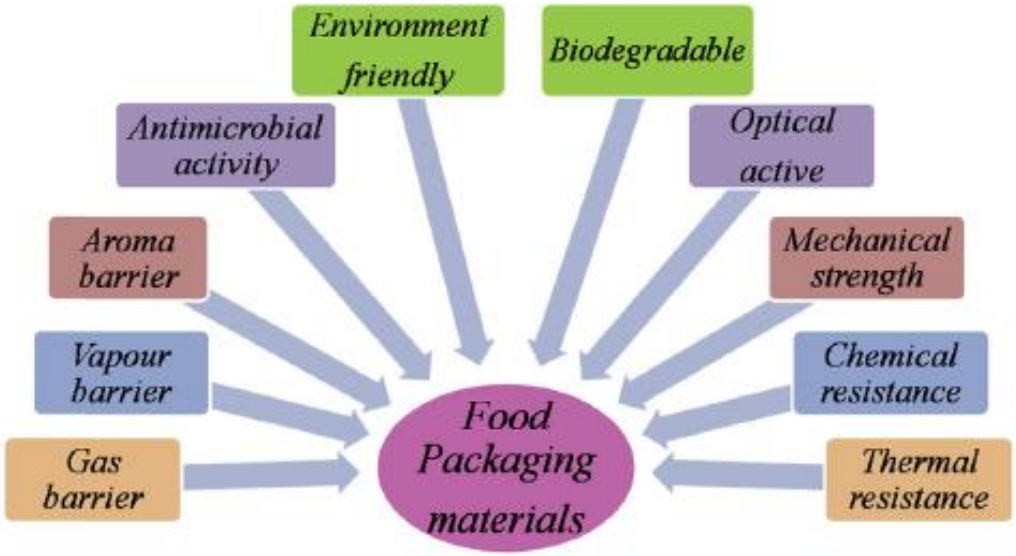

Figure 3 Properties of food packaging materials [4]

1.4.4 Biodegradable Packaging:

Waste disposal is becoming a serious concern for the environment due to limited landfill sites which are diminishing quickly. As an alternative to traditional plastics, compostable and biodegradable polymers have increased in recent years. It is recommended to use biodegradable packaging, having good mechanical strength and barrier properties, particularly as a short term waste management.

1.4.5 Food Packaging Regulation:

The objective of food packaging regulations is to safeguard the buyer from food contamination due to packaging components. It has resulted in a great attention in developing advanced analytical methods for detecting volatile compounds at lower concentrations as well as transferring packaging components at different conditions.

1.5 Active Packaging:

The packaging mode in which high quality of product is maintained by interaction among product, package and the environment which utilizes the incorporation of active agents is called active packaging [11].

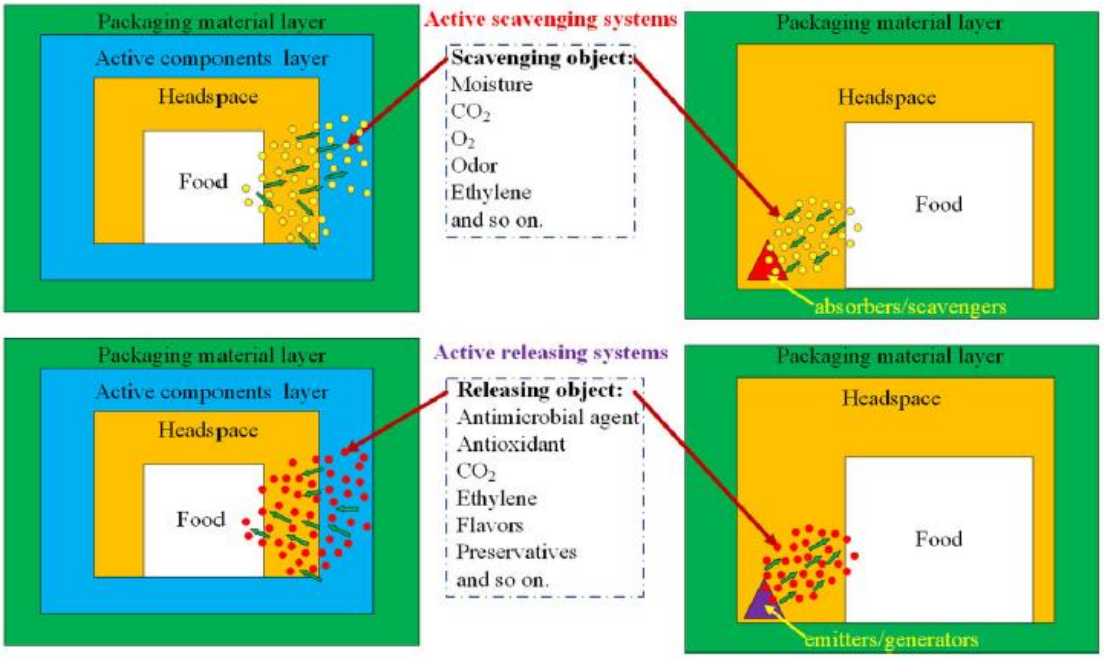

Figure 4 Schematic Diagram of Active Packaging Systems [12]

This involves addition or release of active components, like preservatives, to packaging materials. Few examples of active packaging agents are given below:

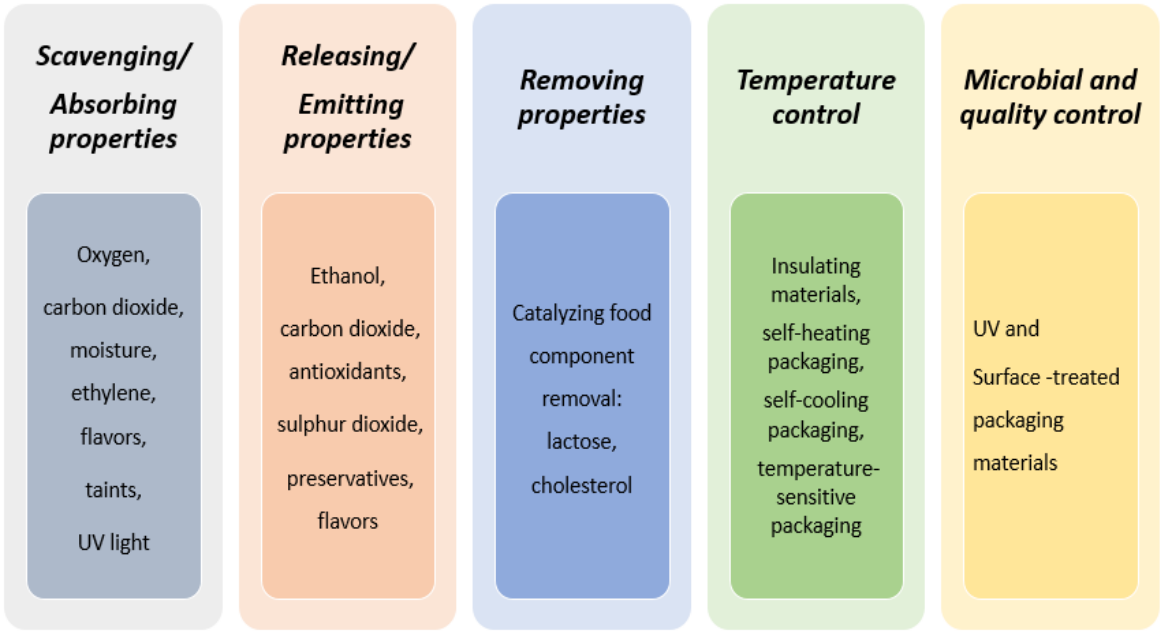

Figure 5 Examples of active packaging agents used in the food industry [13]

1.6 Intelligent Packaging:

Intelligent packaging is focused on technologies capable of processing, evaluating and/or monitoring environmental variations within the container, temperatures during transport and processing, and the microbial food quality[3]. The indicators should be triggered quickly to display an improvement that is quantifiable and permanent, time- and temperature-dependent adjustments should be consistent and preferably associated or accurately associated with food quality, as well as data about the product status.

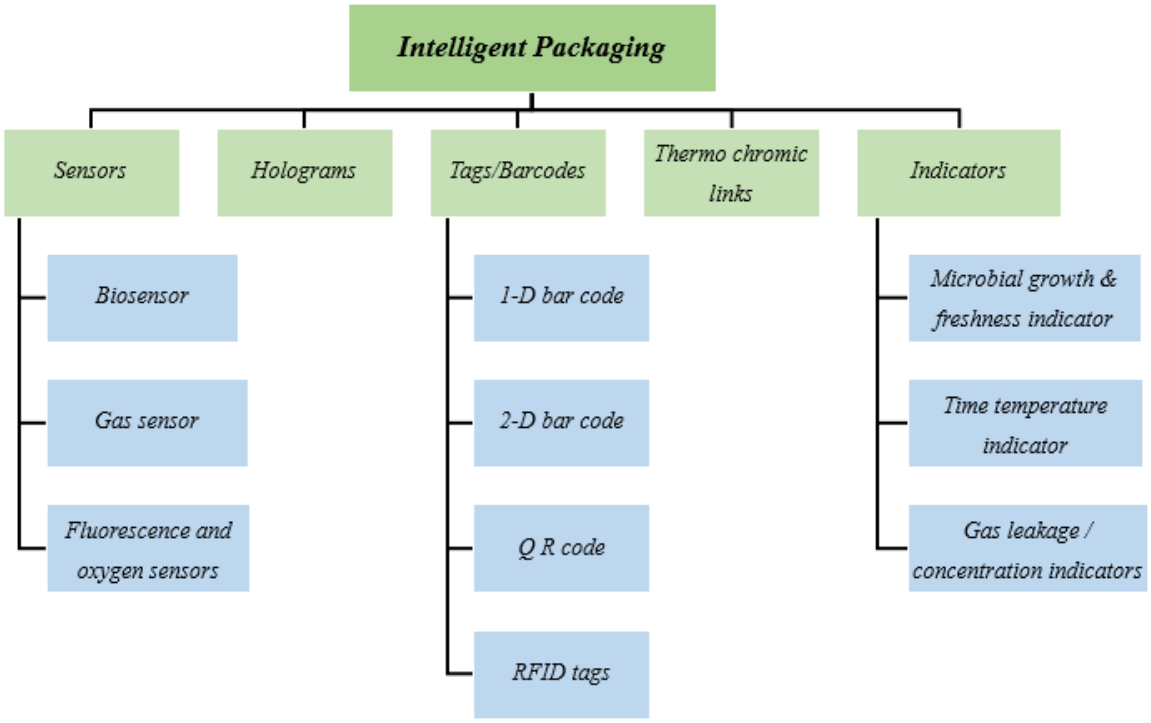

Figure 4 Types of intelligent packaging systems [14]

1.7 Problem Statement:

The evolving technology of efficient and smart biodegradable food packaging has taken over public demands for healthy and safe food with a long shelf life. Nowadays, the most important issue of utilization of biodegradable film as food packaging is the materials employed to synthesize the biodegradable film. Different materials are being utilized in research on the biodegradable films. Bio-polymers are one of the sharp materials utilized for these bio based materials. Bio-polymers obtained from natural resources like proteins, lipids and polysachharide have ended up as the most suitable candidates to form this biodegradable film a short time ago.

Nevertheless, biopolymers utilized in food packaging products have significant problems with their thermal, mechanical and barrier properties, which are quite low in comparison to their traditional equivalents, like petroleum-inferred materials. Various attempts were carried out to improve the characteristics of biopolymers with the principle of nanotechnology that reduces the intrinsic shortcomings of packaging materials.

In this work graphene oxide, in situ reduced graphene oxide(IrGO) and ex situ reduced graphene oxide (XrGO) will be added respectively in PVA /starch membrane to study how the physical, mechanical, thermal and barrier properties of the films get affected.

1.8 Objectives:

Objectives of this research includes:

- To develop carbon based nanocomposite films for packaging applications.
- Physical, thermal and mechanical characterization of nanocomposite films.
- Comparison of in-situ and ex-situ carbon based nanocomposite for packaging films.

Chapter 2

Literature Review

2.1 Biodegradable polymers:

The global biodegradable packaging industry is a tiny fragment, primarily oriented towards innovative and reliable wrapping, whose extremely important portion is biodegradable packaging. The increasing demand for biodegradable packages in conjunction with rising environmental concern contributes to a significant increase in the market as a whole. Food packaging products made up of biopolymers can readily be degraded leaving behind by-products such as CO_2 and H_2O.

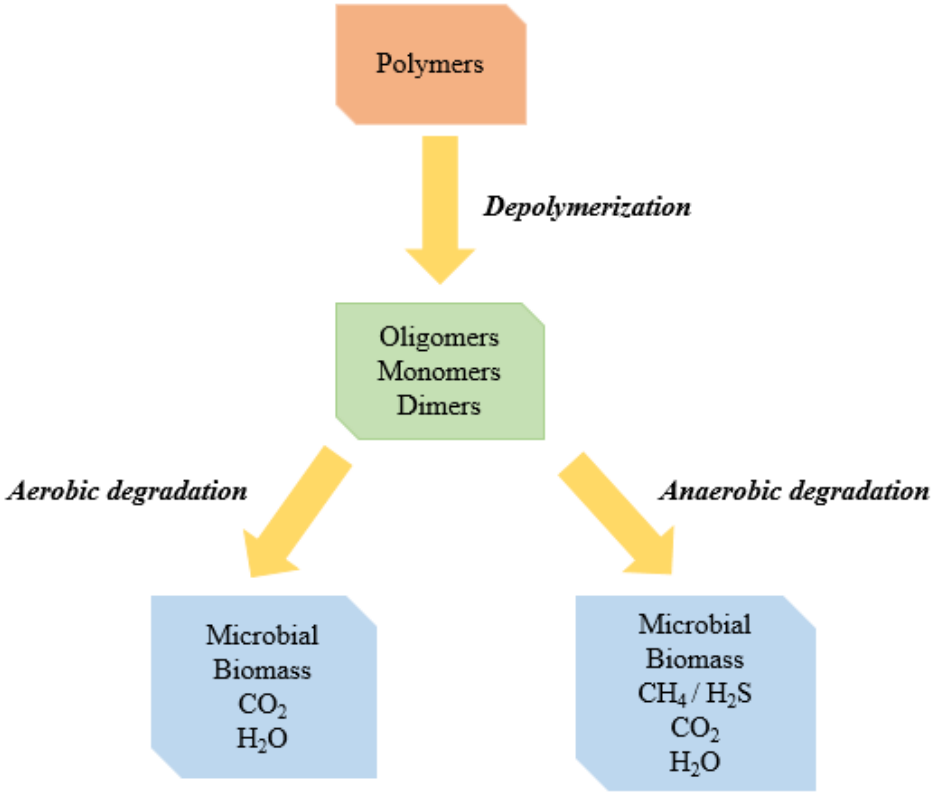

Figure 5 Biodegradation scheme of polymers [15]

2.2 Classification of biodegradable polymers for food packaging:

Based on their origin there are three categories of polymrs i.e. natural, synthetic and modified natural polymers.

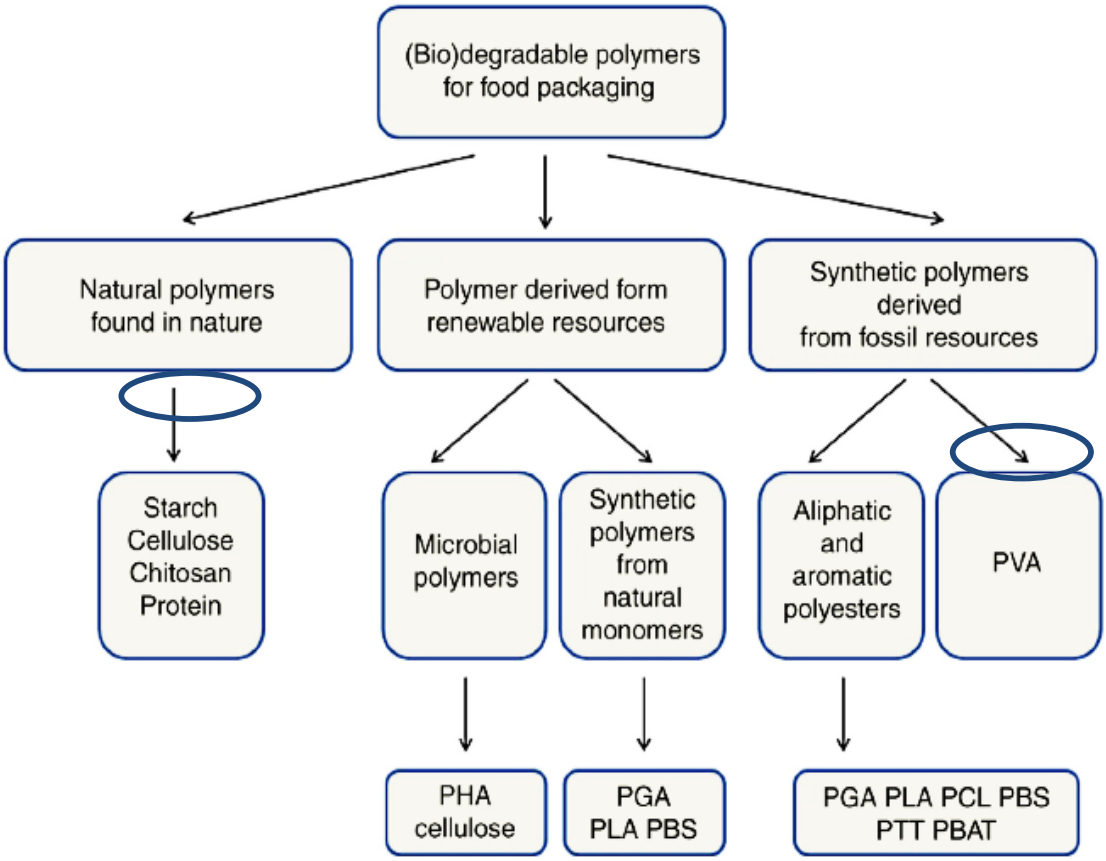

Figure 6 Biodegradable polymers for food packaging [9]

2.2.1 Natural Polymers:

Because of their common root, all natural polymers are biodegradable. There is depolymerase for each polymerase reaction that can facilitate the degradation in order to conserve nature adjustment [9, 16, 17]. Natural items and their derived compounds play a significant part in food packaging industry. Benefits of these polymers include biodegradability, additional nutritive value, antioxidant and antimicrobial properties, renewable sources, reduced cost, universality and having no adverse effect on the atmosphere as a conventional plastic material [9, 18].

2.2.2 Polymers derived from fossil fuel resources:

Polymers derived from fossil fuel resources provide far more benefits as compared to natural polymers. They are modifiable to provide broad variety of properties and adaptable to be utilized for a particular application. These polymers are naturally inert, having anticipated properties, and the raw materials used to produce these polymers are freely existing.

2.2.3 Polymers derived from renewable resources:

Polymers obtained from renewable resources are further subdivided in two groups: one containing microbial polymers and other containing synthetic polymers from natural monomers. In which the former are produced by bacteria and the later are synthesized by polymerization of natural monomers both being the renewable resources.

2.3 Poly Vinyl Alcohol (PVA):

PVA is water soluble, biocompatible, harmless, odor less and biodegradable polymer [19]. It is found in many forms including powder, fiber and films. Moreover, owing to the extraordinary material performance usage of PVA and its blends for packaging application increased vividly. The existence of several hydroxyl groups on PVA surface makes it highly sensitive towards moisture making it popular for packaging applications. PVA is not a totally biodegradable polymer in all situations due to absence of any of the essential requirements, like microorganisms, temperature, pH and relative humidity [20]. Furthermore, number of OH groups on PVA surface affects its biodegradability of PVA.

PVA possess strong molecular interaction owing to its crystalline nature which leads to substantially higher water permeability but quite low oxygen permeability[21]. Krumova et. al [22] reported that adding 3-5% boric acid in PVA leads to enhanced barrier properties owing to the cross linking via new hydrogen bond between hydroxyl groups on boric acid and PVA. Moreover, the permeability was found to be dependent on amount of boric acid.

2.4 Starch:

Starch is an extensively used biopolymer that is actually a plant-based storage polysaccharide. It comprises of both linear and branched polysaccharides, like amylose

and amylopectin [20]. It is among the most plentiful and low cost sources of polysaccharide that has the distinctive characteristic of "biodegradability".

It is considered that starch-based products have drawbacks such as reduced processability and low mechanical properties, weak long-term strength, and increased water sensitivity. These properties have been greatly enhanced by the introduction of numerous synthetic polymers such as PVA, PLA and polyester. Natural sources of starch are rice, potato, wheat, corn etc.

2.5 Need of Polymer blends:

Synthetic polymers with their original form are very difficult to degrade and they keep on adding the waste material into the environment. Global environmental concerns are raising issues against recycling and degradation of plastic polymers. Blending synthetic polymers with purely bio-degradable organic polymers is the new trend which helps the synthetic polymer to partially degrade into the environment through micro-organisms [20]. If natural bio-degradable polymers are used independently, they have no effective use. Blending natural with synthetic polymers results in significant enhancement physical and mechanical properties of the product.

2.6 PVA/starch blends:

PVA is highly compatible with a number of natural polymers such as starch, chitosan, cellulose and lignocellulose when applied for packaging application. Moreover, the compatibility increases in the presence of plasticizer due to increased hydrogen bonding between hydroxyl groups. The influence of three different plasticizers glycerol, sorbitol and citric acid on PVA/starch films is reported by Park et al[23]. The addition of plasticizers resulted in increased solubility of blends as well as elongation at break and decreased the tensile strength.

The effect of various additives like glycerol, succinic acid, citric acid, malic acid, tartaric acid on mechanical properties of PVA/starch membrane has been explored by Yun et al [24]. The reduction in tensile strength and increase in elongation at break was observed by increased amount of additives other than succinic acid which exhibited an entirely opposite trend owing to its hydrophobicity. Generally speaking, the blends are found to

have better physical properties such as odorless, non-toxic, transparent and entirely biodegradable product characteristics although at the cost of minimal mechanical properties.

The increase in starch content in PVA/starch blends leads to improved water vapor permeability due to the hydrophilic nature of starch [25]. Moreover, water vapor permeability can be varied to some extent by altering the storage time [26]. The compatibility and mechanical properties of these blends can be additionally modified by using different cross linkers and additives. Linear rise in water vapor permeability was observed by increasing glycerol content [27].

The biodegradation of PVA blends marginally increased with the increase in molecular weight of PVA whereas higher biodegradability was observed in moist environment [28]. The biodegradability of biopolymers not only depends on the type of microorganisms in soil, components in the blend but also on the compatibility between different components [29]. It was observed during the biodegradation of PVA/starch blend in the presence of glycerol as a plasticizer that the microorganisms completely consumed starch, glycerol and the amorphous phase of PVA; leaving behind the crystalline phase of PVA [30].

2.7 Graphene oxide (GO):

GO was first synthesized by Brodie, in 1859, by oxidizing graphite flakes in nitric acid with potassium chlorate [30]. He further confirmed that graphene oxide contains carbon, hydrogen and oxygen. L. Staudenmaier, in 1898, boosted the degree of oxidation of graphene oxide by adding graphite flakes and potassium chlorates to a mixture of concentrated sulfuric acid and nitric acid [31]. In 1958, alternative synthesis approach for graphene oxide was given by Hummer [32], employing addition of concentrated sulphuric acid and nitric acid over mixture of graphite flakes and sodium nitrate. These all methods result in release of toxic gases like NO_2, N_2O_4 and ClO_2. Improved hummer's method is employed in this work which has certain advantages, like no evolution of toxic gas, more oxidized and regular graphene oxide than that produced by Hummer's method.

Graphene oxide contains oxygenated functional groups like carbonyl, carboxyl, hydroxyl and epoxy groups at the edges of its surface [34]. Thus, making it easy to disperse in water

due to their hydrophilicity. GO and its derivatives like reduced graphene oxide have flourished as the most desirable nanofillers, owing to significant improvement of thermal, mechanical and electrical properties and in addition having good compliance with polymer blends.

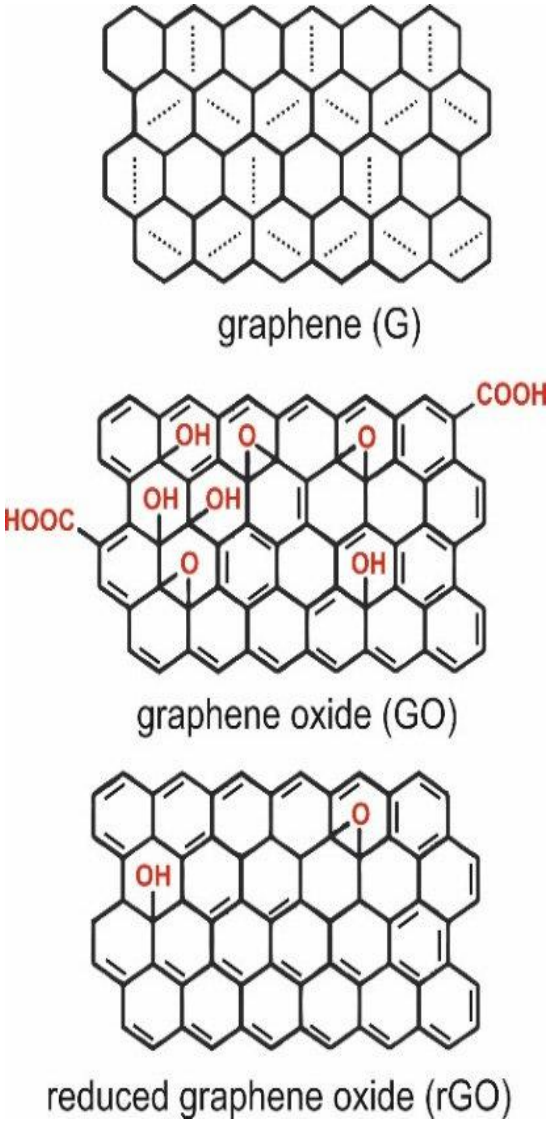

Figure 7 Structure of G, GO and rGO [35]

Figure 8 Comparison of synthesis methods of Graphene Oxide [33]

2.8 Reduced graphene oxide (rGO):

In-depth research has been carried out to synthesize materials having properties close to pristine graphene by elimination of oxygen functional groups from GO by chemical, electrochemical or thermal means [36, 37]. Chemical reduction can be done by adding chemicals like ascorbic acid, hydrazine hydrate, sodium borohydride, dimethyl hydrazine, hydrogen iodide and hydroquinone etc.

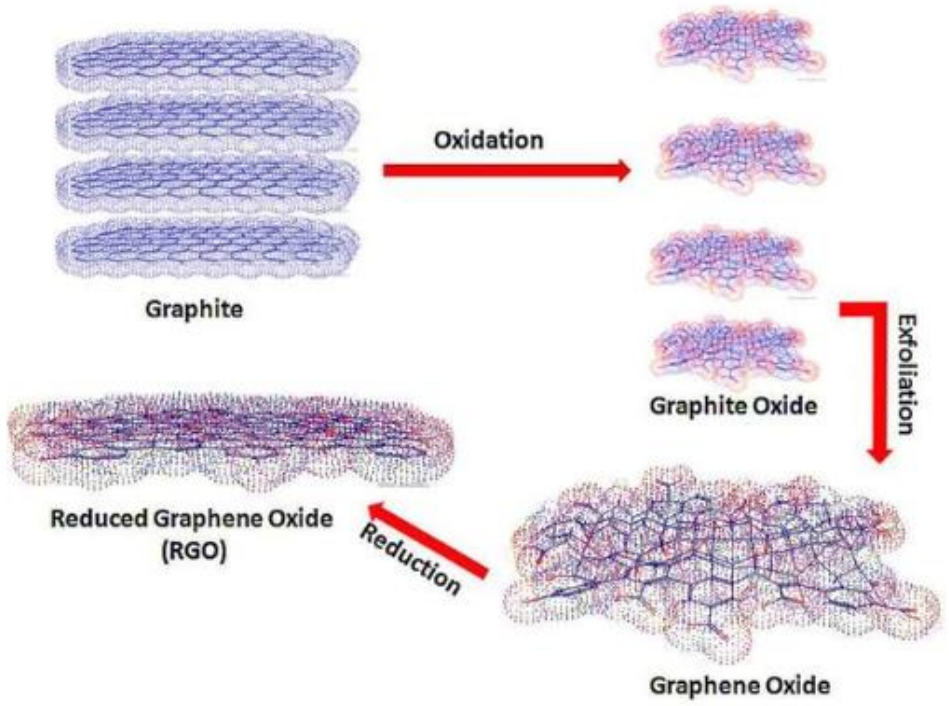

Figure 9 Fabrication of GO and rGO from graphite [38]

2.9 PVA/GO blends:

The degree of oxidation plays a significant role in the structure and properties of GO which eventually affects the properties of GO nanocomposites [39]. Liu et al. [40] varied oxidation degree of GO by changing the amount of $KMnO_4$ which is oxidant. An increase in the degree of oxidation leading to an increase in elongation at break and tensile strength. Incorporation of GO in PVA has been reported in different papers and films were prepared mainly by solution casting [41-43], layer by layer self-assembly [44] and vacuum filtration [45, 46]. Jiaojiao Ma et al.[47] gave a novel approach "insitu polymerization" to synthesize PVA/GO nanocomposites having improved mechanical and water vapor

barrier properties. It was found that adding 20% of GO as filler resulted in a massive increase in tensile strength i.e more than five times of the strength of neat PVA [48]. PVA/GO nanofibers were prepared by electro spinning method [49, 50]. Incorporation of chitosan into PVA/GO nanofiber resulted in enhanced physical, mechanical and antibacterial properties [51].

2.10 PVA/rGO blends:

Rade et al [52] synthesized different types of PVA/rGO nanocomposites including films, hydrogel and colloid dispersion having enhanced mechanical, thermal and biological properties compared to pure PVA. PVA fiber was reinforced with reduced graphene oxide using OPC as a reductant resulting in a considerable enhancement in mechanical properties [53]. PVA/rGO mats prepared by electrospinning [54] having enhanced mechanical and thermal stability were applicable in packaging and tissue engineering.Siyuan Xie et al. [55] synthesized UV shield of PVA/rGO by irradiating with gamma rays.

Chapter 3

Materials & Methods

3.1 Materials:

Poly vinyl alcohol (Degree of Polymerization = 1500), ethanol (97% by wt.), starch, glycerin and hydrochloric acid (31% aq. soln.) were purchased from Daejung Korea. Concentrated Sulfuric acid (98%) was bought from Scharlau Spain. Sodium thiosulfate ($Na_2S_2O_3$) and Sodium Hydroxide (NaOH) were obtained from Merck Germany. Potassium Iodide (KI) was acquired from Ridel-de-Haen. Graphite flakes, Phosphoric acid H_3PO_4 (87%), Potassium Permanganate ($KMnO_4$), $NaNO_3$, H_2O_2, Manganese Sulfate and Sodium Azide were obtained from Sigma Aldrich USA.

All the reagents were of analytical grade and were used as received. The bacterial strains of *Escherichia Coli (E. Coli)* and *Staphylococcus aureus (S. aureus)* were supplied by Atta ur Rehman School of Applied Biosciences (ASAB), National University of Sciences and Technology (NUST), Islamabad. Distilled water has been utilized throughout the synthesis process.

3.2 Synthesis of GO through Improved Hummers Method:

There are various methods which are employed for the synthesis of graphene oxide. In this research, *"improved hummers method"* [56] was used as no toxic gas is formed during the synthesis route. Moreover, Graphene oxide formed by aforementioned process is more oxidized and owns a more regular structure [56].

In this technique, graphite flakes (1 wt. equivalent,3g) and $KMnO_4$ (6 wt. equivalent, 18 g) were added in a beaker. A blend of conc.H_2SO_4/H_3PO_4 was added in a ratio of 9:1 (360ml:40ml) generating a slight exotherm to 35-40 °C was mixed in the same beaker. The mixture was then warmed to 50 °C and left for overnight stirring. After 12 h, the mixture's temperature was lowered to ambient temperature and transferred onto 400ml ice having 3ml hydrogen peroxide (30%) added to it. The mixture was centrifuged at 4500rpm for 4h and the supernatant was emptied each time.

The residual solid material was then washed in sequence with 200ml distilled water, 200ml of 30% hydrochloric acid and then with 200ml of ethanol (2x). After each wash,

the mixture was centrifuged and the supernatant was emptied. After this prolonged washing, the pellet was washed multiple times with distilled water and centrifuged each time followed by decanting the supernatant until the pH~7. After this 200ml of ether was added to the pellet as coagulant after which centrifugation and decanting of supernatant was repeated. The final pellet was dried in petri dish in vacuum oven at 25 °C.

3.3 Synthesis of thermally reduced graphene oxide:

The externally reduced graphene oxide powder was synthesized by using *"thermal reduction of graphene oxide"[57]*. A flask containing 650mg of GO powder covered with aluminum foil having several holes on it was heated in oven at 350°C for about 10 minutes. The black powder obtained was reduced graphene oxide.

3.4 Synthesis of membranes:

Four different membranes i.e. PVA/St, PVA/St/GO, PVA/St/IrGO and PVA/St/XrGO were synthesized during the research. The method of membrane synthesis is explained further in detail.

3.4.1 Synthesis of PVA/St membranes:

5g PVA was dissolved in 85ml of water in beaker by overnight stirring. 1g starch was dissolved in 5ml of water in another beaker and heated to 90 °C for 15 min and then added to PVA solution after being cooled. 1ml of glycerin was added with continuous stirring for another 30mins. After which the solution was pour in petri dish and left for drying at room temperature. Afterwards, the membranes were stripped off and stored in air tight pouches.

3.4.2 Synthesis of PVA/St/GO membranes:

5g PVA was dissolved in 95ml of water in beaker by overnight stirring. 1g starch was dissolved in 5ml of water in another beaker and heated to 90 °C for 15 min and then added to PVA solution after being cooled. GO dispersion was made by varying the amount of GO in mg (10, 20, 30, 40) in 10ml of distill water. GO was dispersed by ultra-sonication for 1h and transferred to the beaker containing mixture of PVA and starch and stirring was continued. 1ml of glycerin was added with continuous stirring for another 30mins. After

which the mixture was casted in petri dishes and kept at room temperature for drying. Afterwards, the membranes (GO) were stripped off and stored in air tight pouches.

Table 1 Membrane formulation methodology

Sr. No.	PVA (g)	Starch (g)	GO (mg)	In situ rGO (mg)	Ex situ rGO (mg)
1	5	1	----	----	----
2	5	1	10	----	----
3	5	1	20	----	----
4	5	1	30	----	----
5	5	1	40	----	----
6	5	1	----	10	----
7	5	1	----	20	----
8	5	1	----	30	----
9	5	1	----	40	----
10	5	1	----	----	10
11	5	1	----	----	20
12	5	1	----	----	30
13	5	1	----	----	40

3.4.3 Synthesis of PVA/St/IrGO membranes:

The synthesis procedure of these membranes was same as section 3.4.3. After adding glycerin and giving it time to mix properly the mixture was placed in an autoclave and kept in oven for 1 h at 120℃. After giving enough time to cool naturally the mixture was poured in petri dishes and kept at room temperature for drying. Subsequently, the membranes (IrGO) were transferred in air tight pouches after peeling.

3.4.4 Synthesis of PVA/St/XrGO membranes:

The synthesis procedure of these membranes was same as section 3.4.3 except GO dispersion rGO dispersion was made by varying the amount of rG0 in mg (10, 20, 30, 40) in 10ml of distill water. The dispersion was made by ultra-sonication for 1h and transferred to the beaker containing mixture of PVA/starch and stirring was continued. 1ml of glycerin was added with continuous stirring for another 30 mins. After which the mixture was casted in petri dishes and kept at room temperature for drying. Later, the membranes (XrGO) were peeled off and put in air tight pouches.

3.5 Characterization Techniques:

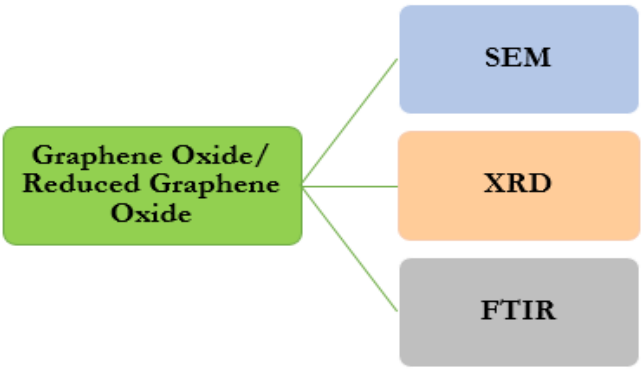

Figure 10 Characterization techniques for graphene oxide & reduced graphene oxide

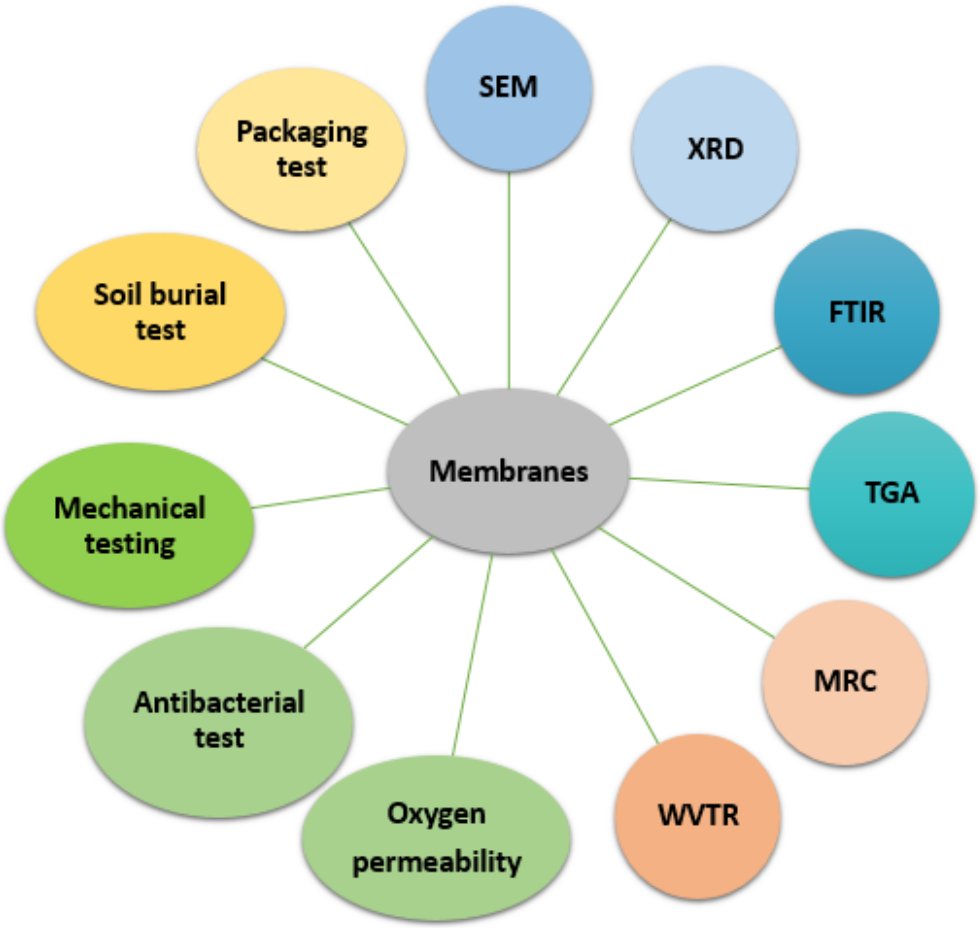

Figure 11 Characterization of synthesized membranes

3.6 Scanning Electron Microscope:

Scanning Electron Microscope (S-4700 Hitachi, Japan) was employed for the morphological study of carbon based nanocomposite membranes. Gold sputtering of 250 Angstrom was done on membranes to cancel charge on it by Ion Sputtering Machine JFC-1500 of JEOL Ltd. Surface of sample was analyzed via a secondary electron detector consuming 5-20kV accelerating voltage.

The key components of SEM are enlisted below:

a) **Electron gun:** Thermionic heating produces electrons at the source which are then quickened to a voltage between 1-40 kV and condensed into a contracted beam which is utilized for analysis along with imaging. The common type of electron sources employed are:

- Solid state gun
- Tungsten filament
- Field emission gun

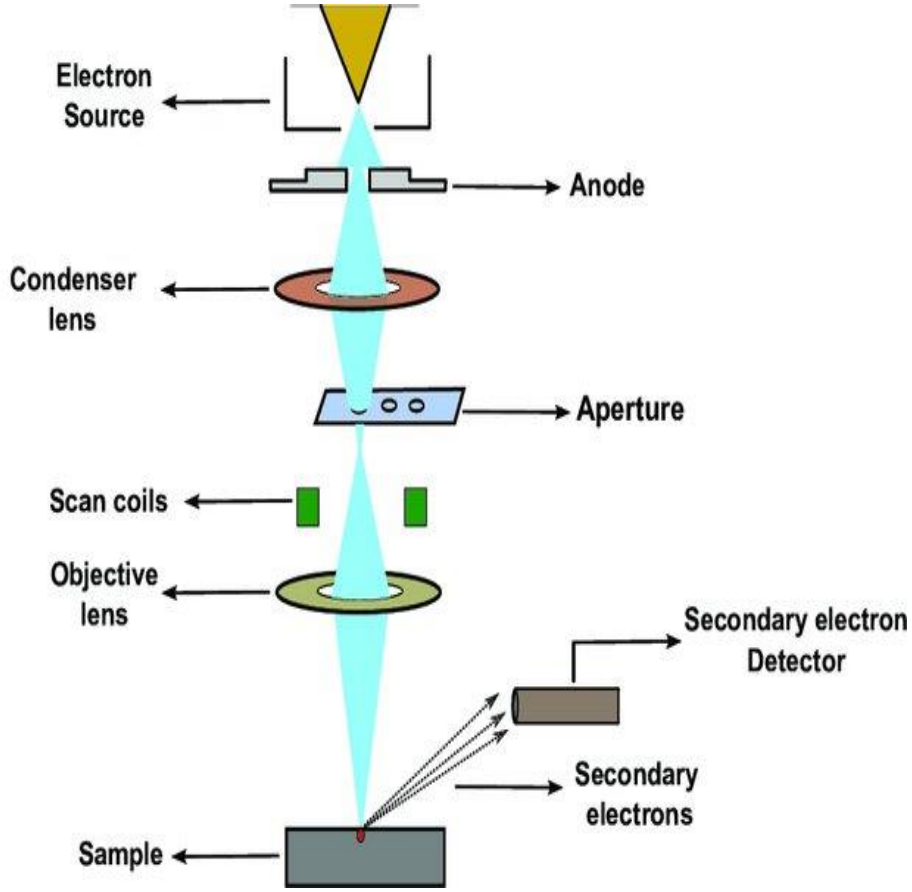

Figure 12 Components of SEM [58]

b) Lenses: Lenses generate clear and detailed images. They are made of magnets instead of glass and can bend the path of electrons. These govern the electron beam by precisely focusing where it needs to go. Basically there are two types of lenses; *Condenser lens* is the first lens that the electrons encounter as the move toward the sample and it sketches the resolution while *Objective lens* focuses the beam on the sample.

c) Sample Chamber: This is where a sample under examination is placed. This chamber must be cut off from vibration and sturdy for keeping the sample still to produce clear images. Sample chamber also moves the specimen at different angles to take different images without constantly remounting the object.

3.7 X-Ray Diffraction (XRD):

The X-ray Diffraction manufactured by STOE-Germany was used to investigate the presence of crystalline materials. The X-ray source has a voltage and current of 40mV and 40mA. The samples were scanned at a 2θ ranged from 5° to 40°. The wavelength of CuKα radiation was 1.540 Å.

Basic elements of XRD are:

1. X-ray tube
2. Sample holder
3. X-ray detector

When the filament is heated electrons are produced, generating X-rays in cathode ray tube. When voltage is applied, accelerated electrons are forced towards the target which gets bombarded with the electrons. The characteristic X-ray spectrum is created when electrons get adequate energy to extract electrons from inner shell of target material.

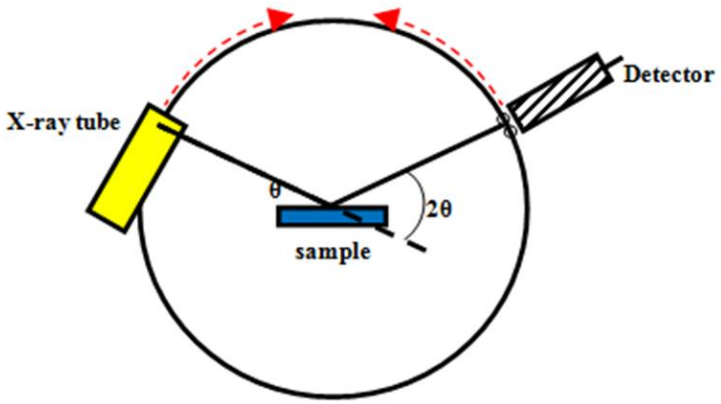

Figure 13 Components of XRD [59]

The Debye-Scherrer Equation was used to approximate the average crystallite size.

$$D_p = \frac{K\lambda}{\beta cos\theta}$$

Where,

D_p is the average crystallite size,

K is the Scherrer constant whose value fluctuates from 0.68 to 2.08, $K = 0.94$ for spherical crystallites with cylindrical geometry,

λ is wavelength of X-rays,

β is the full width at half maxima,

θ is the Braggs angle.

In 1912, Max revealed that the crystalline substances serve as three-dimensional diffraction grills for X-ray wavelengths corresponding to spacing in the plane. XRD is commonly employed to analyze the atomic spacing, crystal structure, material's crystallinity and to distinguish between amorphous and crystalline form.

The constructive interference between monochromatic X-rays and crystalline specimen provides basis for XRD analysis. Cathode ray tube produces X-rays that are filtered so that they can generate monochromatic radiations. These rays are concentrated by collimation and then focused towards the specimen. As a consequence of interaction between these rays and specimen, constructive interference provided Bragg's law is satisfied which relates wavelength of the electromagnetic radiations to the lattice spacing and diffraction angle of the specimen. It is mathematical expressed as:

$$\boldsymbol{n\lambda = 2d \sin \theta}$$

Where,

n = reflection order,

λ = wavelength of X-rays,

d = spacing among crystal planes of a given sample

θ = angle formed between incident beam and that normal to the lattice plane.

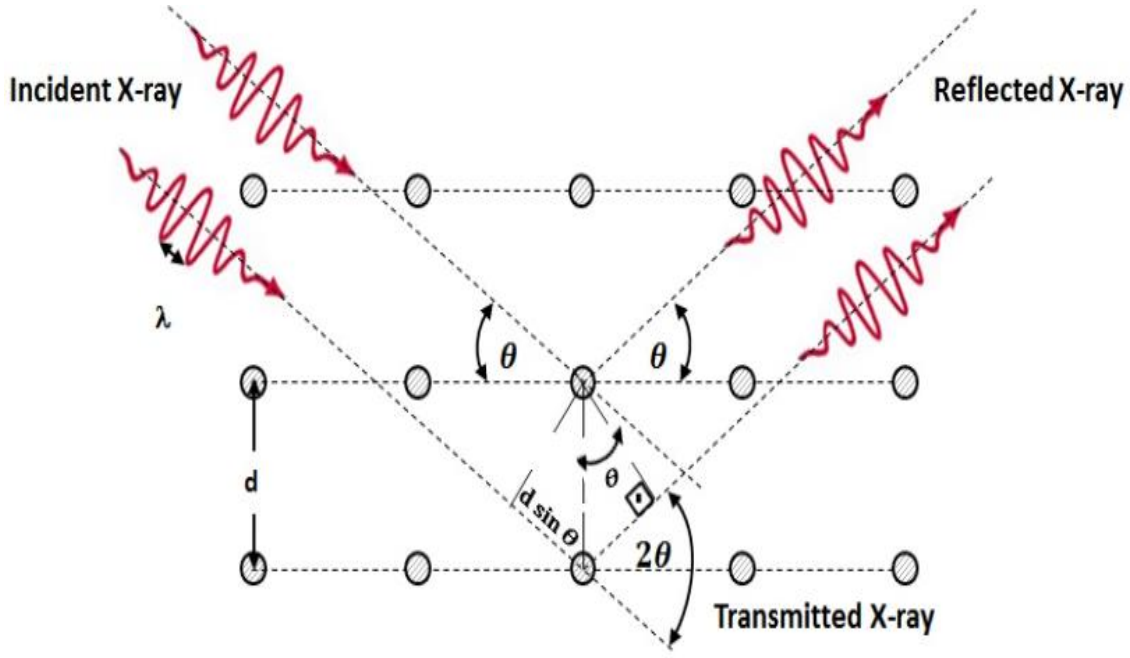

Figure 14 Schematic Diagram of Bragg's Law [60]

3.8 Fourier Transform Infrared (FTIR) Spectroscopy:

Fourier Transformation Infra-red spectroscopy is done to inspect the existence of chemical bonds in any material via absorbance or transmittance spectrum. Incoming light beam is divided via beam splitter in two discrete light paths, half of the beam is reflected and half is transmitted. The transmitted beam moves to a fixed mirror and the transmitted light travel from moving mirror recombines at the beam splitter, then leave the Michelson inferometer and then travels through the sample and reaches the detector. Each bond present in the specimen absorbs specific energy as it vibrates at a specific frequency. The sample can be powder, membrane or even liquid. Fourier Transform is the mathematical algorithm that collects the absorption data and analyze it.

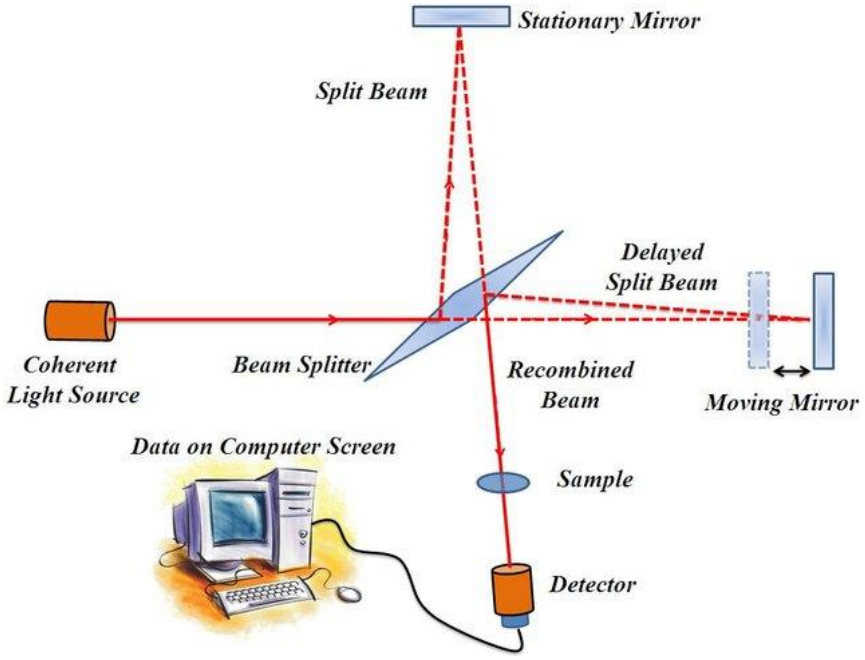

Figure 15 Components of FTIR [61]

For alkanes, there are two bonds; C-C, C-H bonds. Of which the vibrations of C-C bond occur in finger print region while that of C-H bonds are observed at around 2800-3000 cm^{-1}. Alkenes have C=C other than having C-H bond, the C=C stretching vibration occurs around 1600-1800 cm^{-1}. For Alkynes, the C≡C bond vibrations occur around 2000-2300 cm^{-1}. The vibration of nitrile group i.e. C≡N occurs at around 2100-2300 cm^{-1} while the vibrations of carbonyl group C=O and imine group C=N are found at 1500-1800 cm^{-1}. The vibration of O-H group i.e. hydroxyl group occurs around 3200-3600 cm^{-1} whereas N-H stretch occurs at around 3500-3700 cm^{-1}.

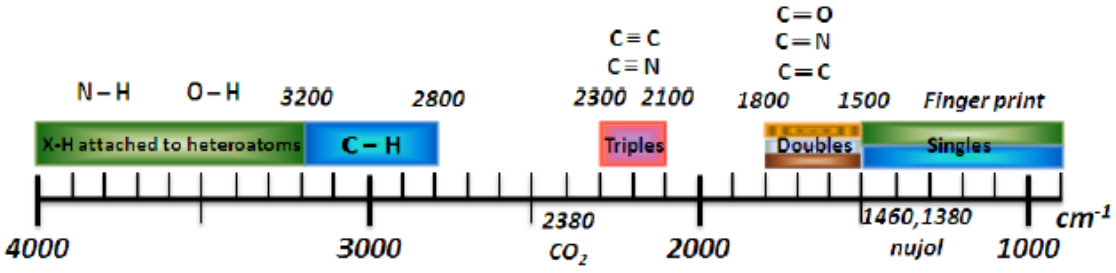

Figure 16 Different bonds stretching regions in FTIR spectra [61]

3.9 Thermal Gravimetric Analysis (TGA):

TGA is the technique used to analyze changes in weight with change in temperature of the sample. The sample is heated in the presence of nitrogen or using air as an atmosphere from ambient temperature to high temperature at a constant heating rate. Different weight loss steps in the decomposition profile can be accredited to different components in the sample, like water, solvent or membrane's degradation. The components of TGA are:

1. Balance
2. Furnace
3. Programmer for temperature control and measurement
4. Recorder for temperature as well as mass variations

The balance is required to ensure reproducibility, accuracy and sensitivity. The linear heating over a wide temperature range is provided by the furnace. Typically, it varies from -150℃ to 2000 ℃. Thermocouples measure and regulate the temperature. Commonly, there are two thermocouples. One is used to measure temperature change while the other activates the control system. The recorder unit performs the function of digital data acquisition and records measurements.

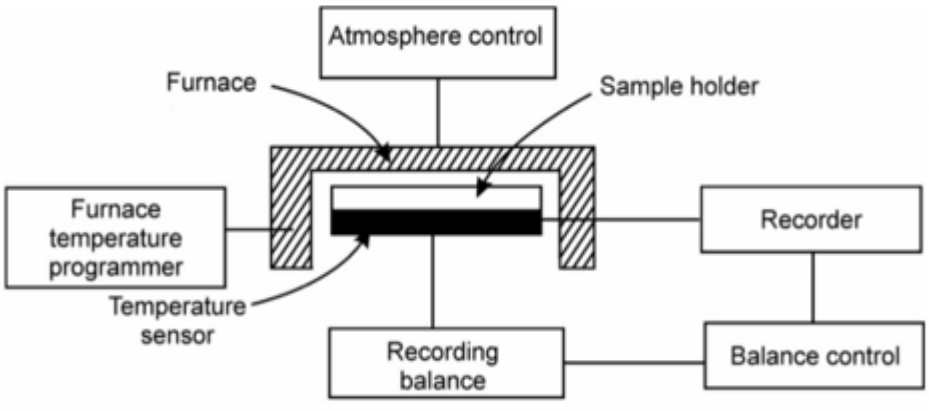

Figure 17 Schematic Diagram of TGA [62]

3.10 Mechanical Testing:

Mechanical properties of the membranes were investigated by assessing the elongation at break and breaking stress employing Trapezium-X Universal Testing Machine (AG-20RRKNXD Plus) assembled by Shimadzu Cooperation. Samples were cut in rectangular shape having dimensions of 50x10 mm^2 and the analysis was done at a cross head speed of 50mm/min and gauge length was set to be 30 mm. The thickness of every sample was measured individually.

Figure 18 Mechanical Testing Machine

Tensile strength (TS) was calculated using following formula

$$TS = {}^{F}/_{A}$$

F (N) is applied force and A (mm^2) is initial area of film sample.

Percentage Elongation (%E) is calculated as:

$$\% E = {}^{l - l_i}/_{l} \times 100$$

l_i (mm) is the initial length of sample film, l (mm) is the final length of sample film.

3.11 Moisture Retention Capacity:

To evaluate the moisture retention capacity, membranes were cut in 1x1 cm^2 and initial weight W_i was measured. The membranes were then kept in oven for 6 h at 40 ℃ after which final weight W_f is measured. The percentage moisture retention capacity was calculated via the formula

$$\%\, \boldsymbol{MRC} = \left(\frac{\boldsymbol{W_f}}{\boldsymbol{W_i}}\right) \times \mathbf{100}$$

W_i was the initial weight and W_f was the final weight after placing in oven.

3.12 Water Vapor Transmission Rate:

To complete estimations of water vapor transmission, a media bottle with mouth measurement 29.5 mm was used. 10 ml of distilled w ater was poured in it and the mouth was sealed with the membrane by using Teflon tape. The initial weight was measured and then the bottle was kept in oven at 40 ℃ for 24 hr. Subsequently, the bottle was removed from the oven and its final weight was calculated.

The water vapor transmission rate was calculated by utilizing the formula:

$$\boldsymbol{WVTR}\ \left(\boldsymbol{g}/\boldsymbol{m^2 h}\right) = \frac{\boldsymbol{W_i - W_f}}{\boldsymbol{A \times 24}} \times \mathbf{10^6}$$

Here W_i and W_f were the initial and final weight of the bottle respectively. *A* was the area of circular mouth of bottle.

3.13 Oxygen Permeability Test:

The oxygen permeability of membranes was measured using “Winkler Method”. Media bottles were filled with water; covered with membranes and sealed with the help of Teflon tape. These were then stored for a period of 24 hr. Afterwards, the bottles were analyzed for dissolved oxygen. One bottle was kept open and the other was closed to approximate the oxygen permeability in case of positive and negative control respectively. The values were expressed in mg/ml.

The highly accurate method for determining the amount of dissolved oxygen in water, was evaluated by analytical chemist Lajos Winkler in 1888. The protocol is as follows:

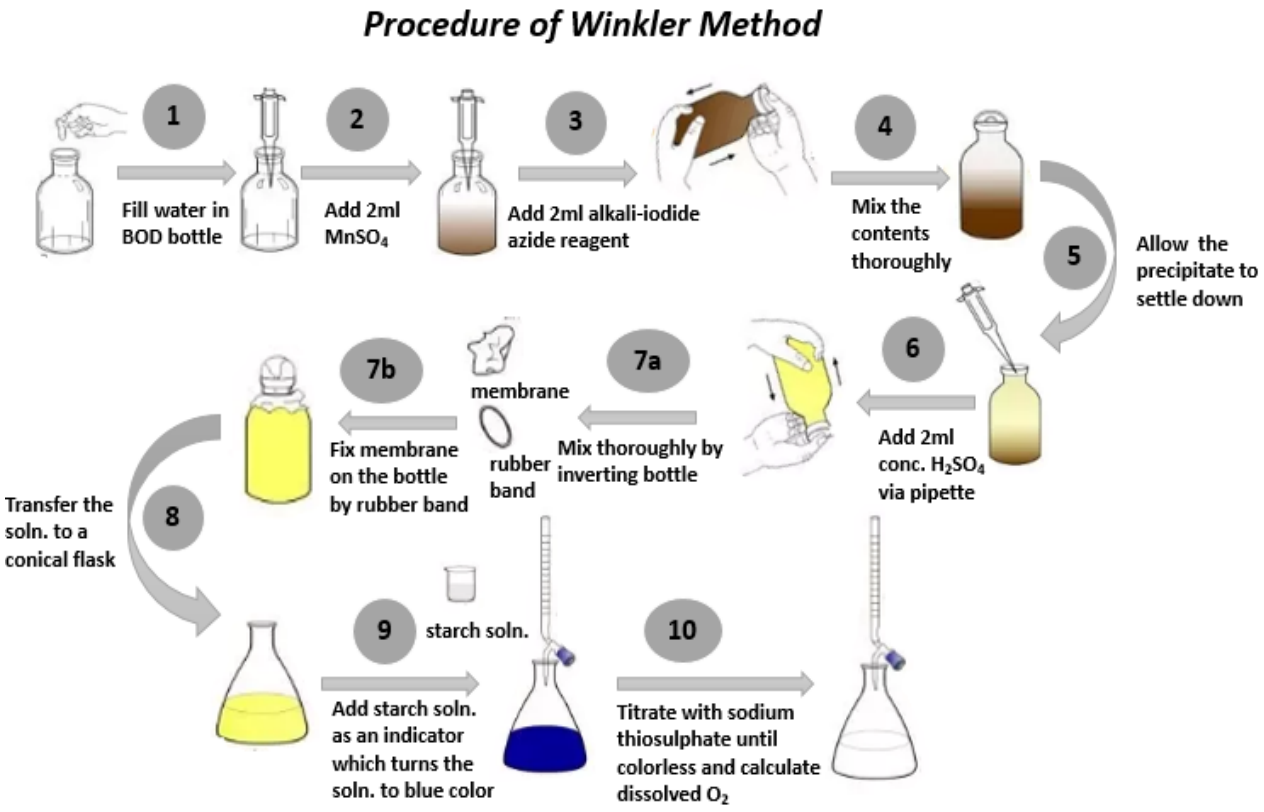

Figure 19 Winkler's Method for Oxygen Permeability

Oxygen permeability was calculated by the formula:

$$\mathbf{O_2} = \frac{\mathbf{V_1} \times \mathbf{N} \times \mathbf{E} \times \mathbf{1000}}{\mathbf{V_4}(\mathbf{V_2} - \mathbf{V_3})/\mathbf{V_2}} \left({}^{mg}/_{ml}\right)$$

Where,

V_1=Volume of titrant $Na_2S_2O_3$ (ml)

V_2=Total volume of water specimen (ml)

V_3=Volume of ($MnSO_4$+KI) reagent added (ml)

V_4=Volume of analyte taken for titration (ml)

E=Equivalent weight of O_2

N=Normality of $Na_2S_2O_3$ solution

3.14 Antibacterial Test:

The antibacterial activity of membranes against two common food born bacterial strains i.e. *E. Coli* and *S. Aureus* was measured by ***"Agar Well Method"***. 1.6 g broth was added in 200 ml of distilled water and shaken well to make it homogenous. Then, 10 ml of solution out of this bottle in to test tube and 1 ml of *E.Coli* strain is added to it. Followed the same procedure for *MRSA* strain. These test tubes were placed in shaking water bath for 18 to 24 hours at 37°C, so the bacteria in the test tube grow and the broth solution becomes cloudy.

The agar solution was made by adding 7 g of agar in 250 ml of distilled water and then homogenized by shaking. Then the agar solution was poured to petri dishes and permitted to solidify. These petri dishes were then stacked and covered with the food wrap and placed in incubator. After 24 hours these plates were removed to see any contamination. If no contamination was found, then the bacteria grown broth was evenly spread over the agar plates. Afterwards holes of 6mm size were punched in each plate followed by adding the 6mm discs of prepared nanocomposite films. The agar plates were then again wrapped in food wrap and placed in incubator at 37°C for 16hrs followed by measuring the zone of incubation. All the media bottles, agar soln., LB broth, petri dishes, spreader used were autoclaved first to kill all other bacteria.

3.15 Food packaging test:

Phyllanthus emblica was chosen as a fruit to test for the applicability of food packaging. PVA/St, PVA/St/GO, PVA/St/IrGO and PVA/St/XrGO membranes were employed for the testing. During testing the fruit was packed in membranes and sealed with Teflon tape. The fruit packed was free from defects and two of the goose berries were kept in open environment as the control. The percent weight loss was calculated on everyday basis to check the shelf life of product [63].

3.16 Biodegradation Test:

The biodegradation test was carried by indoor burial of membranes. Natural organic soil was added in the container having dimensions 10x5x6 cm^2 to be utilized as a system for

the test. Initially the samples were cut in rectangular shape with dimensions 1x2 cm^2 accompanied by drying in oven at 60℃ for 4 hrs. Samples were then placed and buried in soil at a depth of 4 cm. Soil was watered daily to maintain uniform conditions. The percentage weight loss of films was checked the next day with the help of following formula as a parameter to measure degree of degradation.

$$\boldsymbol{percentage\ weight\ loss} = \left[\frac{\boldsymbol{m_i - m_f}}{\boldsymbol{m_i}}\right] \times \mathbf{100}$$

m_i was the initial mass and m_f was the mass left after burial of membranes.

Chapter 4

Results & Discussion

4.1 XRD Analysis Results:

X-ray diffraction was done using X-ray powder diffractometer (XRD STOE θ-θ Germany).

4.1.1 XRD Result of GO:

Figure 20 demonstrates the XRD results of GO. XRD of pure graphite has a peak at 26° as reported in literature [64, 65]. Oxidation of graphite to synthesize graphene oxide results in peak shifting. Strong diffraction peak at 10.84° was observed, with complete disappearance of peak at 26°, which confirmed the successful synthesis of graphene oxide [66, 67]. This kind of change in peak position is well known in literature for GO formation, arising from the presence of oxygen containing functional groups like hydroxyl, carboxyl and epoxide groups [68].

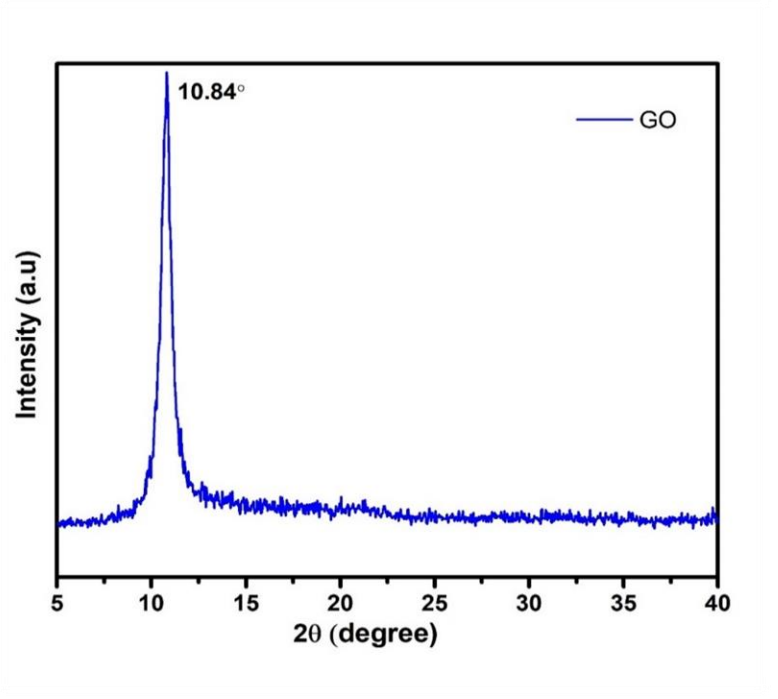

Figure 20 XRD of Graphene Oxide (GO)

4.1.2 XRD pattern of rGO:

Reduced graphene oxide was synthesized by thermal reduction of graphene oxide and its XRD is shown in figure 21. The peak at 10.48° in GO shifted to 24° in rGO due to decrease in oxygen containing functional groups [69, 70]. Broad peak was attributed to a single or a few layers' structure [71] that differs significantly from pristine graphite.

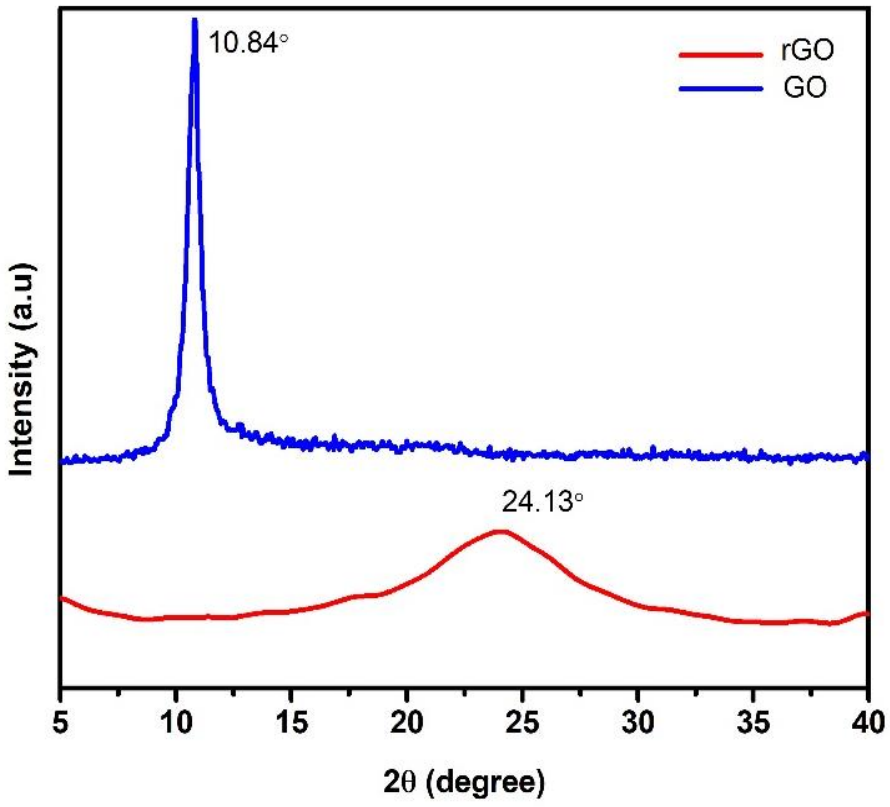

Figure 21 XRD of reduced Graphene Oxide (rGO)

4.1.3 XRD pattern of PVA/St/GO membranes:

XRD of PVA/St and PVA/St/GO membranes is shown in figure 22. The XRD of pure PVA/St membrane shows peak at 19.72° due to the semi crystalline nature of PVA. Upon addition of graphene oxide to the PVA/St membrane there is a slight shift in peak i.e. from 19.7 ° to 19.1 °. No peak broadening or extra peak of graphene oxide was observed showing that the addition of GO has no substantial effect on PVA crystallite size [72].

Moreover, this can be ascribed to a very small amount of GO is added and due to the homogenous dispersion of GO within the PVA matrix [73].

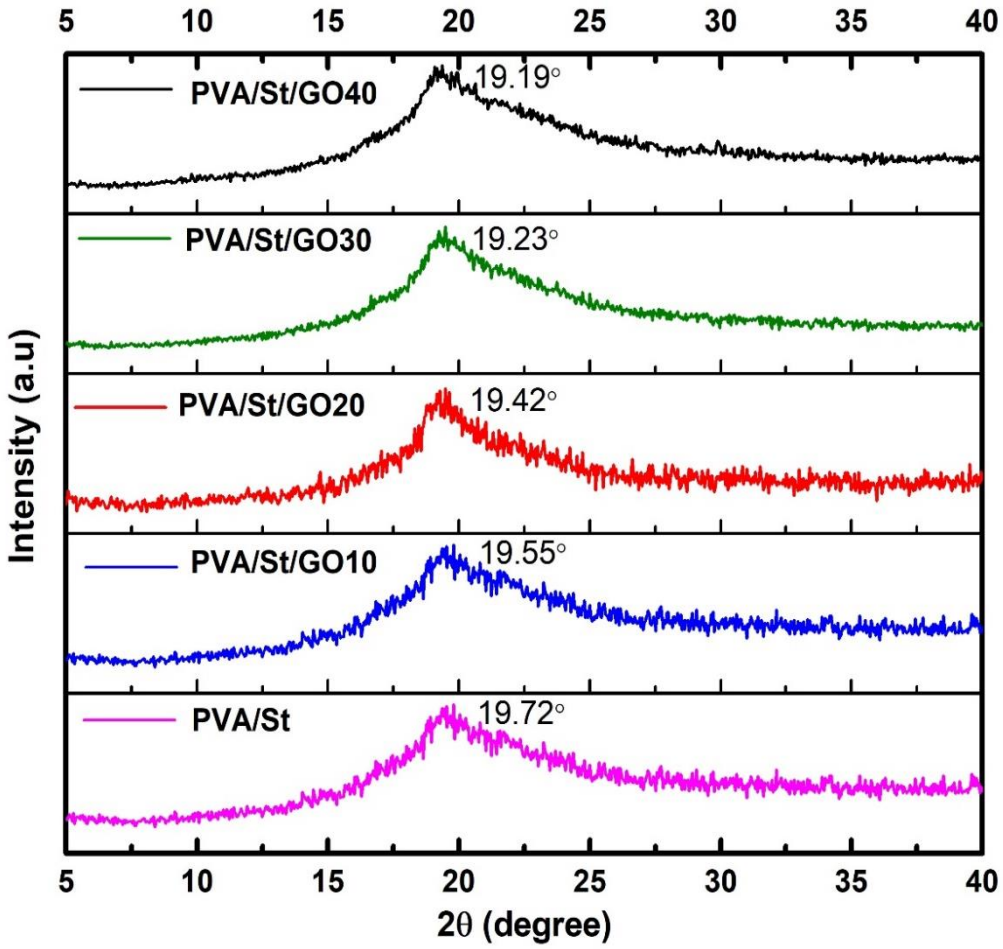

Figure 22 XRD of PVA/St/GO membranes

Furthermore, GO was delaminated well in the PVA matrix owing to the non-covalent bonding between the oxygen containing functional groups in GO with the polymer chain [74].

4.1.4 XRD pattern of PVA/St/IrGO membranes:

XRD of PVA/St/IrGO membrane is shown in Figure 23 a). The XRD pattern shows only the peak at 19^{o} due to the presence of PVA [75, 76]. No extra peak of in-situ reduced graphene oxide was observed due to complete exfoliation and uniform dispersion of IrGO in the PVA matrix. Just a minor peak shift from 19.4 ^{o} to 19.01 ^{o} was seen showing that IrGO has no significant effect on the crystallinity of PVA.

4.1.5 XRD pattern of PVA/St/XrGO membranes:

XRD of PVA/St/XrGO is shown in Figure 23 b). In the XRD only peak at 19º was showing the presence of PVA in the membranes. No extra peak was seen for the (ex-situ) reduced graphene oxide owing to complete exfoliation along with uniform dispersion of XrGO in the polymer matrix.

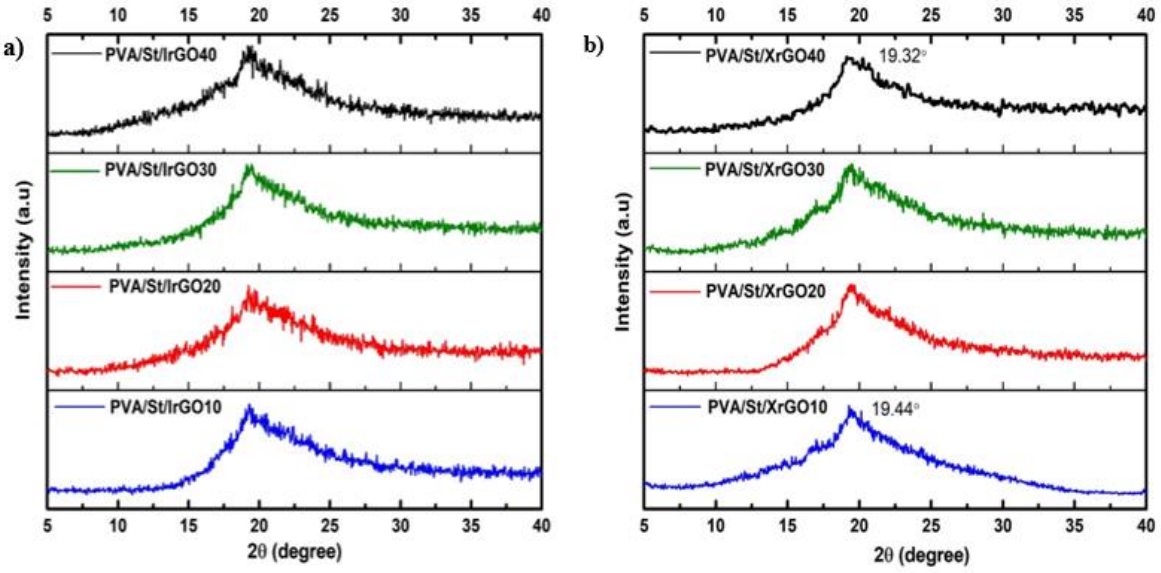

Figure 23 XRD of membranes a) PVA/St/IrGO b) PVA/St/XrGO membranes

4.2 SEM Analysis Results:

SEM analysis was carried out using JOEL-JSM-6490A Japan.

4.2.1 SEM Analysis of GO:

The surface appearance in Figure 24 illustrate that GO has a 2D sheet-like wrinkled structure having lamellar configuration with distinguished edges [77]. Moreover, GO sheets are thicker at the edges because functional groups are majorly present at the edges.

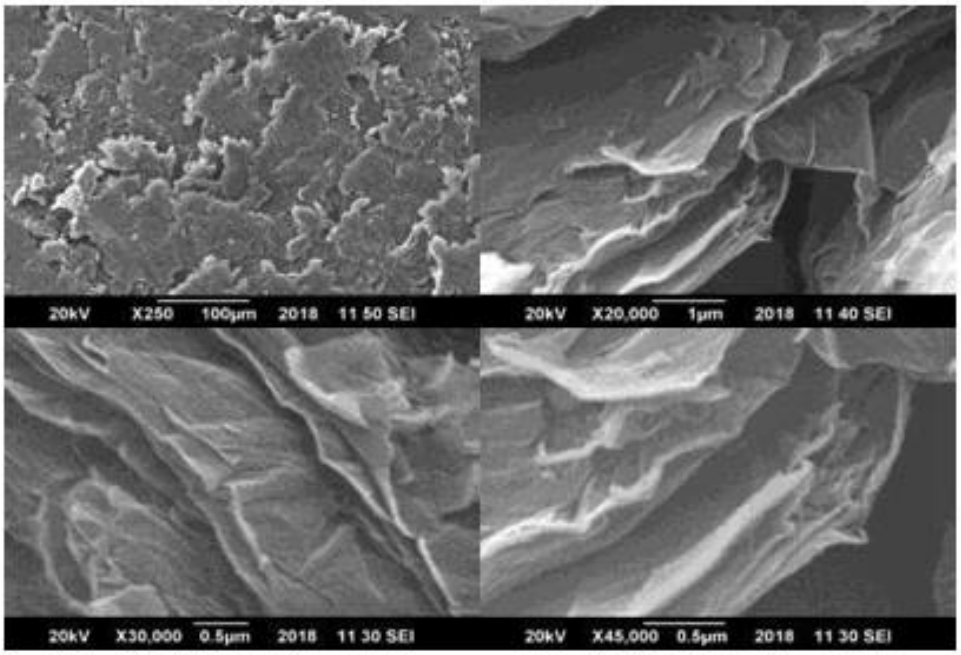

Figure 24 SEM images of GO

4.2.2 SEM Analysis of rGO:

SEM images in Figure 25 reveals that free floating rGO nano-sheets are single or few-layered with 2D membrane like structure and sheets are entangled with each other. Sheets have wrinkled and rippled structure because of exfoliation and restacking processes.

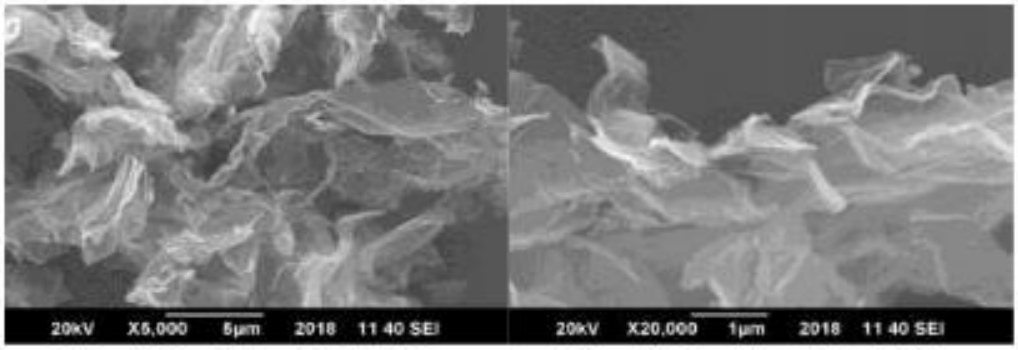

Figure 25 SEM images of rGO

4.2.3 SEM Analysis of PVA/St membranes:

Figure 26 shows the surface appearance and cross section of PVA/St membranes. It was clearly visible that the surface is smooth showing perfect mixing of PVA and starch. The surface gives no indication of pores even at such a high resolution showing that the membrane is dense.[78]

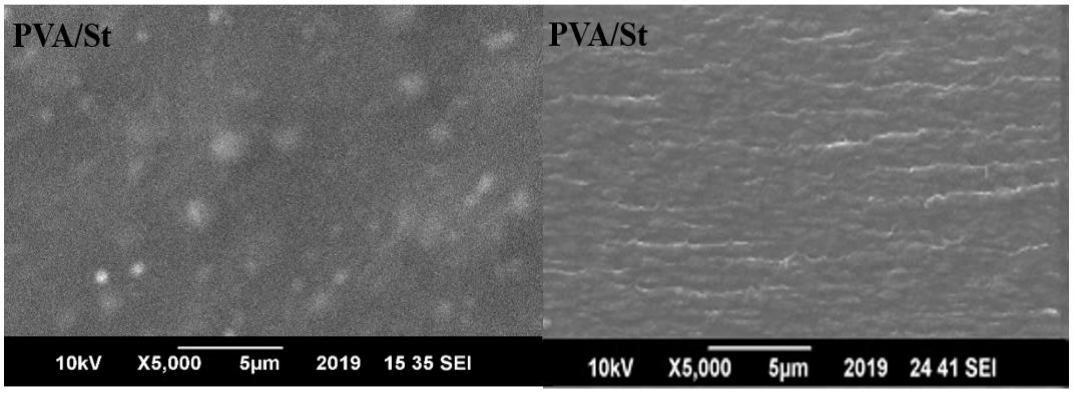

Figure 26 Surface and Cross-sectional SEM of PVA/St membrane

4.2.4 SEM Analysis of PVA/St/GO membranes:

SEM analysis of PVA/St/GO membranes revealed that the incorporation of GO resulted in dense membranes showing uniform distribution of graphene oxide in PVA/St/GO10 as shown in Figure 27.

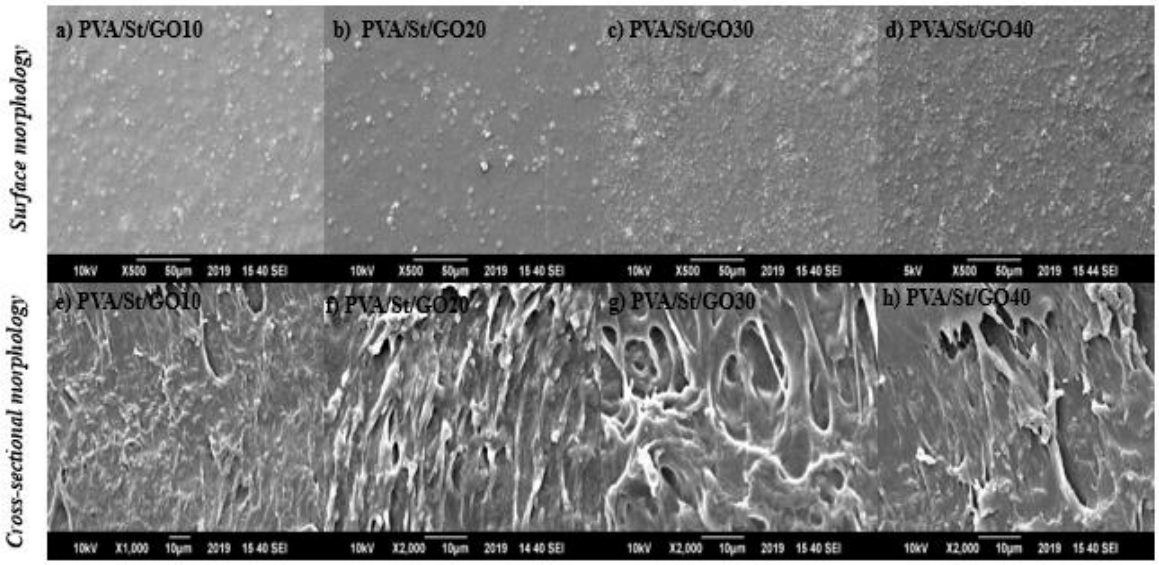

Figure 27 Surface and Crosssectional SEM of PVA/St/GO membranes

The cross-section of all membranes showed that they contain lamellae structure due to presence of graphene oxide. Further increase in amount of GO i.e. 20, 30 and 40 mg clearly showed the presence of graphene oxide in excess on the surface. Also the cross-section of these membranes showed non-uniform weaker lamellae which was further confirmed after mechanical testing.

4.2.5 SEM Analysis of PVA/St/IrGO membranes:

Surface and cross-sectional analysis of PVA/St/IrGO membranes is shown in Figure 28. The surface appearance PVA/St/IrGO20 membrane showed a smooth surface and the membranes containing higher amount of IrGO revealed agglomeration on surface. Moreover, the cross-section showed wrinkled structures exhibiting the successful insitu reduction of graphene oxide. Also the lamellae structure displayed the weakest bonding at PVA/St/IrGO.

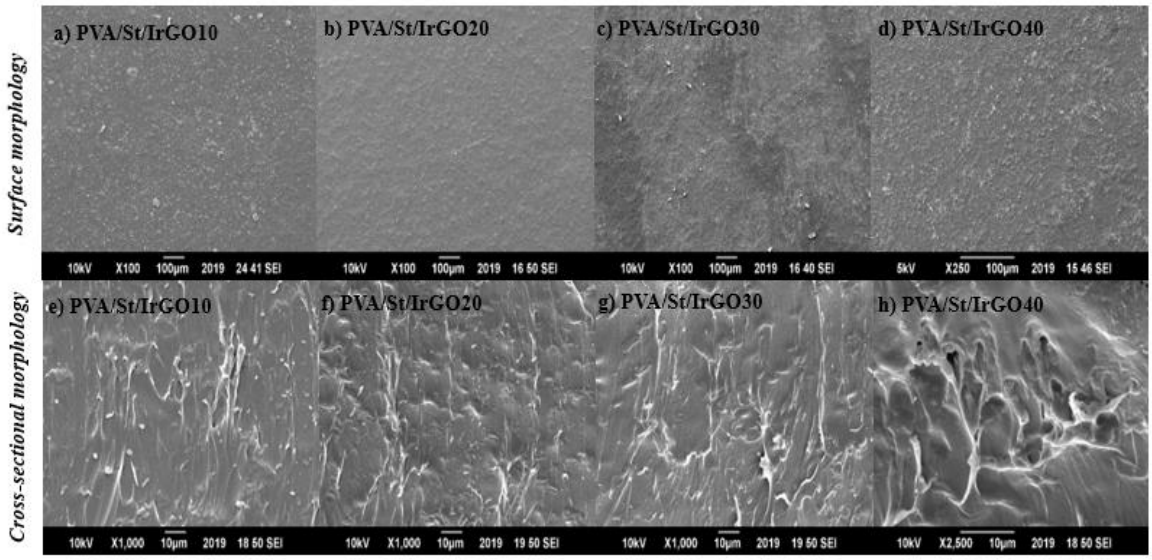

Figure 28 Surface and Cross-sectional SEM of PVA/St/IrGO membranes

4.2.6 SEM Analysis of PVA/St/XrGO membranes:

The surface morphology of PVA/St/XrGO membranes displayed a uniform smooth surface at XrGO10 as shown in Figure 29. Afterwards the surface visibly showed the presence of rGO particles on the surface. Furthermore, crossectional analysis displayed the wrinkled structure confirming the incorporation of reduced graphene oxide within the PVA matrix.

Cross-sectional morphology revealed agglomeration after PVA/St/XrGO10 with huge agglomeration seen in case of PVA/St/XrGO40.

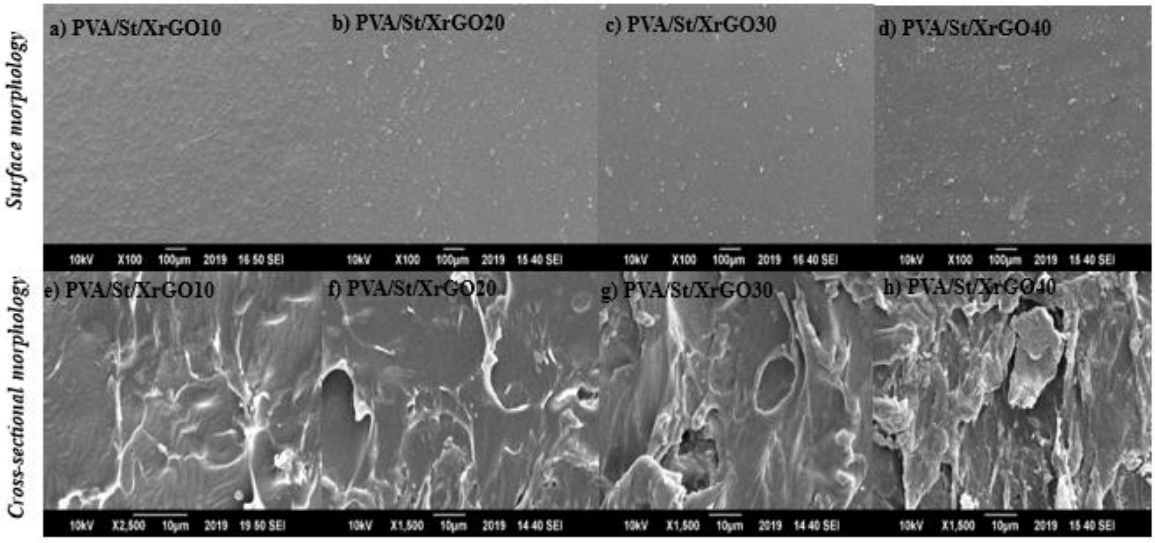

Figure 29 Surface and Cross-sectional SEM of PVA/St/XrGO membranes

4.3 Fourier Transform Infrared Spectroscopy (FTIR):

4.3.1 FTIR Analysis of GO & rGO:

FTIR spectra of graphene oxide is shown in Figure 30. It is well known that there are various functional groups present in GO like hydroxyl, alkene, carbonyl groups [57]. From graph, the peak due to OH stretching vibrations appeared at 3309, while peak due to C-H, C=O stretching vibrations appear at 2101, 1629 [79]. The peaks at 1397, 1275, 1070 and 979 occur C=C, C-OH, C-O-C and C-O respectively [56, 80]. The presence of these functional groups confirmed the efficacious synthesis of GO. During the reduction of GO, the functional groups containing oxygen are removed [57]. From Figure 30, it is clear that the peak due to OH stretching disappeared completely while the peaks due to C-H at 2096 and C=C at 1574 were still there. These results depict the successful synthesis of rGO through GO reduction by noticeable decrease in the attached functional groups.

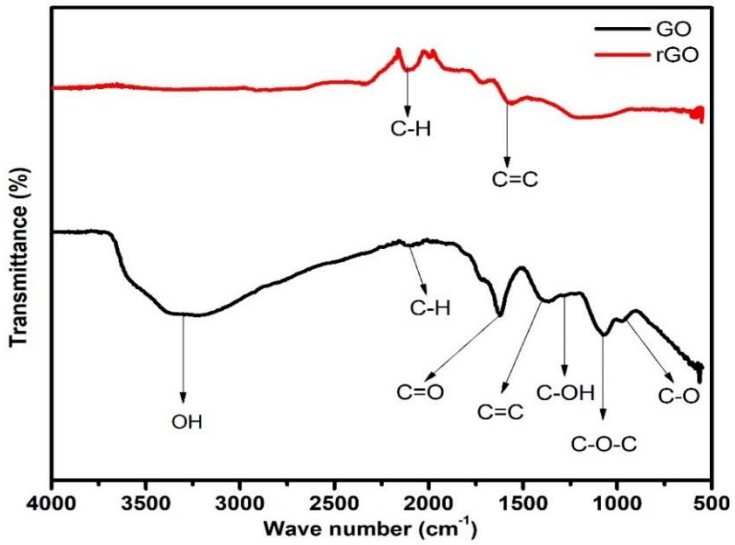

Figure 30 FTIR of GO and rGO

4.3.2 FTIR Analysis of membranes:

FTIR analysis of membranes is shown in Figure 31. The appearance of a broad peak from 3100-3600 cm^{-1} shows OH stretching vibrations due to inter and intra molecular hydrogen bonding among components like PVA, starch, GO [80]. The peak present between 2891-2961 cm^{-1} is attributed to aromatic CH stretching vibrations [79]. The C=O stretching vibrations occur around 1730 cm^{-1} with slight shift possibly due to hydrogen bonding [81].

The peak around 1640 is due to the bound water [82]. The peak at 1430 and 917 is attributed to CH_2 stretching vibrations. Similar results were seen in case of PVA/St/IrGO and PVA/St/XrGO.

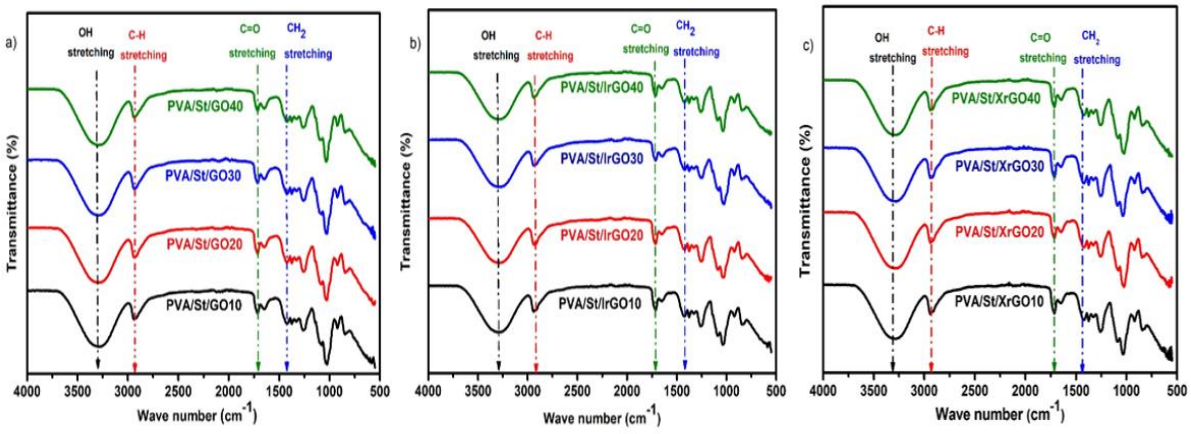

Figure 31 FTIR of membranes a)PVA/St/GO b)PVA/St/IrGO c)PVA/St/XrGO

4.4 Thermal Gravimetric Analysis:

The synthesized membranes were analyzed to check their thermal stability. TGA of the membranes shown in Figure 32 contains different weight loss stages. The first weight loss stage from 30-105℃ is moisture or solvent i.e. water removal [79]. The second weight loss from 105-250℃ exhibits the removal of functional groups like epoxy, hydroxyl and carbonyl groups present in PVA as well as graphene oxide [80]. Afterwards, another major weight loss stage exists from 250-470℃ owing to the decomposition of carbon backbone and oxygen containing functional groups known as carbonization [83].

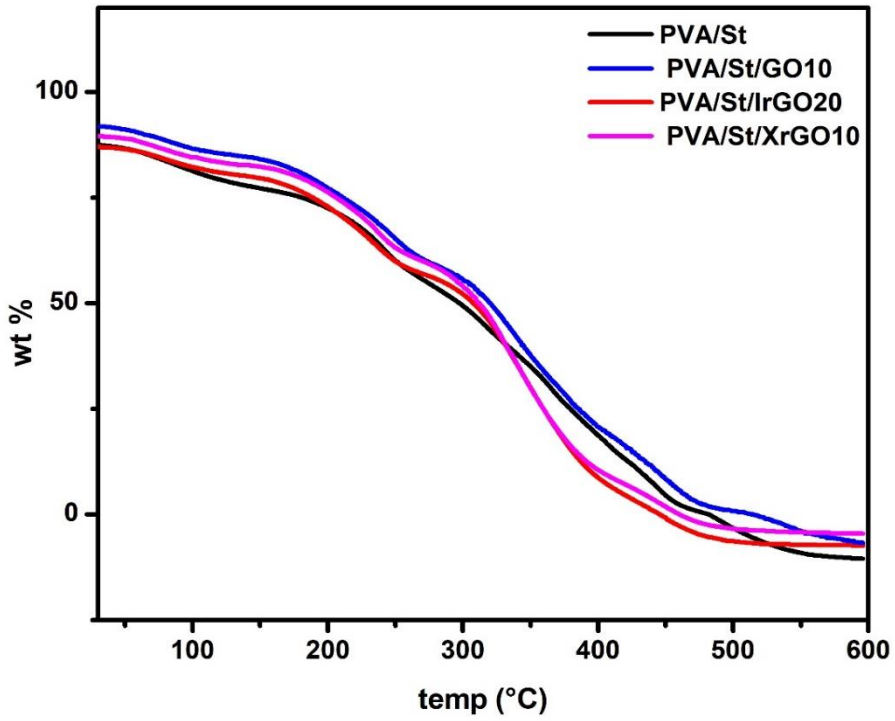

Figure 32 TGA of membranes

After 500℃, there is almost no major weight loss. Moreover, it can be concluded from TGA that the PVA/St/IrGO membrane is thermally more stable as compared to PVA/St, PVA/St/GO and PVA/St/XrGO membranes as the TGA curve of former lies well below the later.

4.5 Mechanical properties:

The mechanical properties of packaging materials are of huge concern. These include tensile strength and percentage elongation; the former shows maximum strength that a material can endure when stretched until failure or breakage occurs whereas the later indicates the maximum stretch that a material can bear. The result of mechanical testing of membranes is illustrated in Figure 33 a) and b) whereas the values are tabulated in table 2.

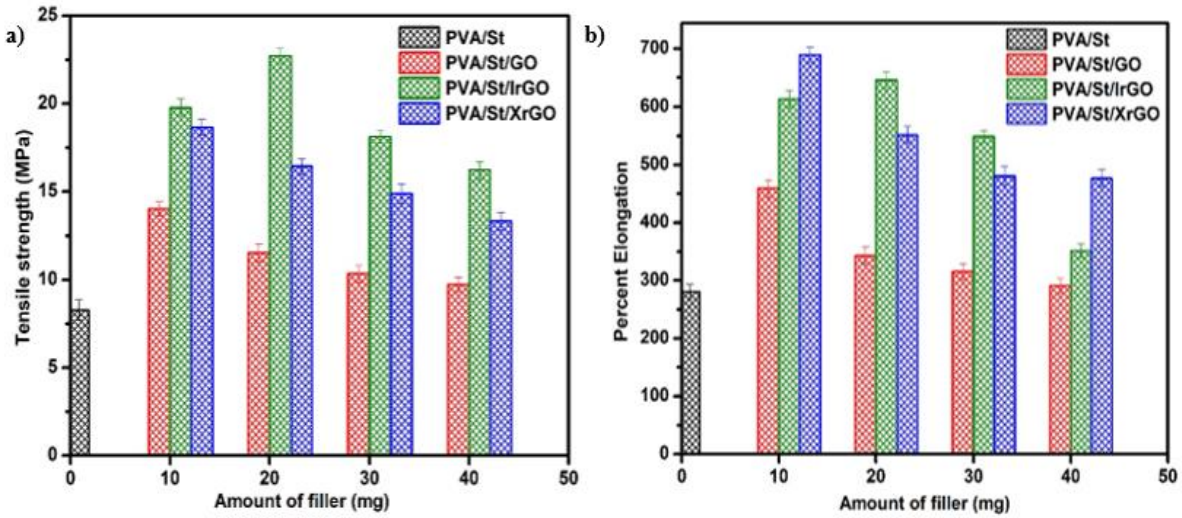

Figure 33 a)Tensile Strength b)Percent Elongation of membranes

Adding graphene oxide to the PVA/St membrane resulted in increase of its tensile strength till the amount of GO was 10 mg after which the strength starts decreasing. Tensile strength of PVA/St/IrGO20 and PVA/St/XrGO10 is maximum and decreases afterwards. The percent elongation of membranes showed that the films containing GO have maximum elongation at GO10. In this case tensile strength and % elongation both are maximum at GO10. Moreover, in the case of PVA/St/IrGO and PVA/St/XrGO the tensile strength and % elongation have similar trends i.e. where tensile strength is maximum the value of percent elongation is also maximum. Overall the tensile strength has maximum value in case of PVA/St/IrGO membrane whereas % elongation is maximum in case of PVA/St/XrGO membrane. These findings are in line with literature [84].

Table 2 Tensile Strength & Percent Elongation of membranes

Sr. No.	Membrane	Tensile Strength (MPa)	Percent Elongation
1	PVA/St	8.26 ± 0.59	280.60 ± 0.69
2	PVA/St/GO10	14.02 ± 0.4	459.42 ± 0.89
3	PVA/St/GO20	11.53 ± 0.51	342.41 ± 0.92
4	PVA/St/GO30	10.35 ± 0.46	314.88 ± 0.78
5	PVA/St/GO40	9.72 ± 0.44	290.41 ± 0.82
6	PVA/St/IrGO10	19.79 ± 0.48	613.32 ± 0.56
7	PVA/St/IrGO20	22.72 ± 0.45	645.96 ± 0.67
8	PVA/St/IrGO30	18.12 ± 0.36	548.66 ± 0.83
9	PVA/St/IrGO40	16.24 ± 0.5	351.05 ± 0.75
10	PVA/St/XrGO10	18.65 ± 0.45	689.02 ± 0.65
11	PVA/St/XrGO20	16.43 ± 0.42	551.04 ± 0.73
12	PVA/St/XrGO30	14.89 ± 0.56	480.45 ± 0.43
13	PVA/St/XrGO40	13.32 ± 0.52	475.87 ± 0.78

4.6 Moisture Retention Capability:

Moisture retention capability reveals the moisture level within the films. Regulation of moisture transfer is essential to preserve the appearance, flavor and overall quality of packaged products. The food packaging films are well known for their high moisture retention capability.

The results of moisture retention capability of PVA/St, PVA/St/GO, PVA/St/IrGO and PVA/St/XrGO membranes are illustrated in Figure 34 a). Test showed that the synthesized membranes have very high and nearly similar values moisture retention capability. These high values are attributed to the OH groups in PVA, starch and glycerin present in each

film which are capable of capturing water. Thus the moisture is locked within the film matrix.

Higher the values of moisture retention capability lower will be the loss of moisture from the films resulting in lesser film distortion. The values of moisture retention capability lie from 87% to 95.8%. These values are in agreement with the moisture level needed in packaged fruits i.e. from 78% to 95% [1].

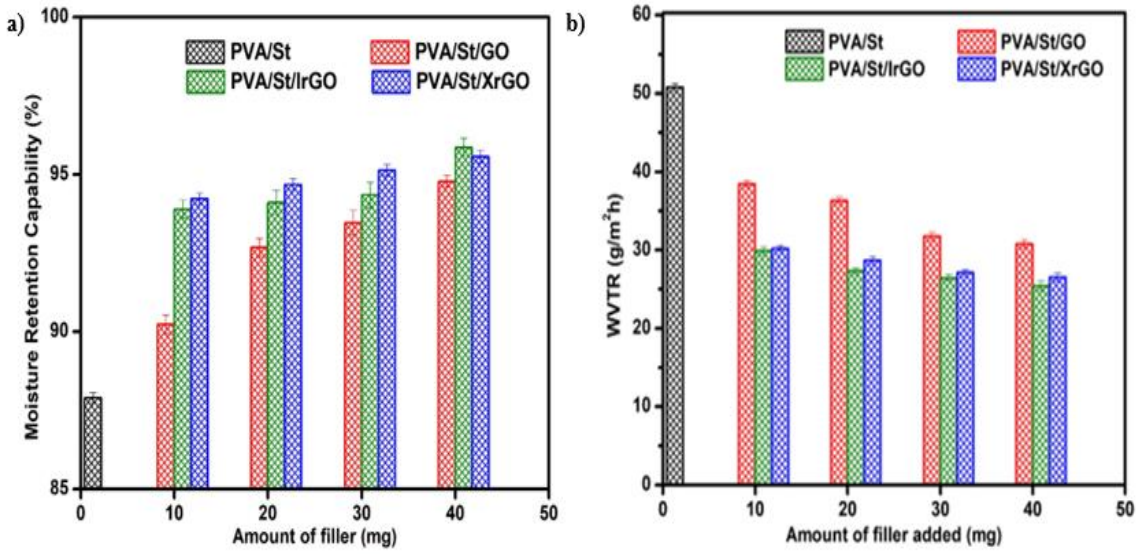

Figure 34 a) Moisture Retention Capability b) WVTR of membranes

4.7 Water Vapor Transmission Rate (WVTR):

The purpose of food packaging is to prevent the outside moisture from entering inside the films. The films possessing lesser values of water vapor transmission rates are applicable as food packaging films since they guarantee protection, better credibility of package and product along with an increased shelf life [85].

Water vapor transmission rate test was conducted to check the applicability of the synthesized membranes in food packaging. The WVTR values of PVA/St, PVA/St/GO, PVA/St/IrGO and PVA/St/XrGO are shown in Figure 34 b).It is well known that the addition of fillers enhances the barrier properties of membranes by providing a torturous path [86] which ultimately results in the decrease in WVTR.

Table 3 MRC and WVTR of membranes

Sr. No.	Membrane	MRC (%)	WVTR (g/m^2h)
1	PVA/St	87.9 ± 0.17	50.8 ± 0.46
2	PVA/St/GO10	90.23 ± 0.29	38.43 ± 0.39
3	PVA/St/GO20	92.68 ± 0.28	36.35 ± 0.42
4	PVA/St/GO30	93.47 ± 0.38	31.76 ± 0.5
5	PVA/St/GO40	94.78 ±0.19	30.78 ± 0.52
6	PVA/St/IrGO10	93.89 ± 0.29	29.9 ± 0.48
7	PVA/St/IrGO20	94.10 ± 0.39	27.34 ± 0.37
8	PVA/St/IrGO30	94.34 ± 0.39	26.48 ± 0.49
9	PVA/St/IrGO40	95.86 ± 0.29	25.43 ± 0.58
10	PVA/St/XrGO10	94.22 ± 0.18	30.22 ± 0.38
11	PVA/St/XrGO20	94.67 ± 0.19	28.68 ± 0.49
12	PVA/St/XrGO30	95.14 ± 0.19	27.14 ± 0.38
13	PVA/St/XrGO40	95.56 ± 0.19	26.56 ± 0.49

The addition of graphene oxide to the PVA/St membrane decreased the water vapor transmission rate as compared to pure PVA/St membrane. In case of internally reduced graphene oxide as a filler in PVA/St membranes the lower values of WVTR were observed due to layered structure of the membranes as proven by SEM. Almost comparable results were achieved in the case of PVA/St/XrGO membranes. Owing to the layer structure by the addition of fillers the water molecules have to follow a torturous path rather than a straight one which results in decreased values of WVTR [87].

4.8 Oxygen permeability result:

The aim of food packaging is to protect shield food from the influence of external environment. Presence of oxygen within the packet can affect food quality, its appearance and taste [88]. Thus the food packaging films should be an excellent barrier against

oxygen. The oxygen permeability across the membranes was measured by "Winkler Method" [89, 90]. The membranes were placed on top of media bottles containing distill water and sealed with Teflon tape. One bottle was kept open and other was closed by cap to be used as positive and negative control respectively [91]. The bottles were left for 12 h after which the dissolved oxygen was measured in mg/ml.

The test involves addition of $MnSO_4$ followed by the addition of NaOH resulting in formation of $Mn(OH)_3$. Moreover, alkali iodide azide reagent was added to correct the presence of nitrite which can otherwise affect the readings [92].

$$4MnSO_4 + 8NaOH \rightarrow 4Mn(OH)_2 + 4Na_2SO_4$$

$$4Mn(OH)_2 + O_2 + 2H_2O \rightarrow 4Mn(OH)_3$$

The Mn^{+3} ions are then acidified by addition of H_2SO_4

$$2Mn(OH)_3 + 3H_2SO_4 \rightarrow Mn_2(SO_4)_3 + 6\,H_2O$$

$$2Mn_2(SO_4)_3 + 4KI \rightarrow 4MnSO_4 + 2K_2SO_4 + 2I_2$$

Starch solution was used as an indicator that turns solution to blue which was then titrated against sodium thiosulphate.

$$4Na_2S_2O_3 + 2I_2 \rightarrow 2Na_2S_4O_6 + 4\,NaI$$

End point of this titration is a clear solution.

Results of this test are shown in Figure 35. Usually the dissolved oxygen in the water lies between 7 to 14 mg/ml [90, 92]. The value of dissolved oxygen of open and closed bottle were 12.1 and 5.29 mg/ml respectively. The value of oxygen permeability across PVA/St/GO ranged between 7.8 to 7.2 mg/ml.

The values of PVA/St/IrGO membranes ranged between 5.68 to 5.35 and that of PVA/St/XrGO membranes ranged between 5.86 to 5.5. These values are somewhat more than the closed bottle but much lower than the open bottle. These results clearly show that

Table 4 Oxygen Permeability of membranes

Sr. No.	Sample	Oxygen Permeability (mg/ml)
1	Open	12.1 ± 0.5
2	Closed	5.29 ± 0.6
3	PVA/St	8.42 ± 0.44
4	PVA/St/GO10	7.89 ± 0.25
5	PVA/St/GO20	7.42 ± 0.35
6	PVA/St/GO30	7.36 ± 0.23
7	PVA/St/GO40	7.2 ± 0.24
8	PVA/St/IrGO10	5.68 ± 0.24
9	PVA/St/IrGO20	5.45 ± 0.34
10	PVA/St/IrGO30	5.39 ± 0.26
11	PVA/St/IrGO40	5.35 ± 0.37
12	PVA/St/XrGO10	5.86 ± 0.26
13	PVA/St/XrGO20	5.79 ± 0.37
14	PVA/St/XrGO30	5.65 ± 0.34
15	PVA/St/XrGO40	5.5 ± 0.26

with the addition of nanofillers the oxygen permeability decreases due to the tortuous path which provides hindrance to the gas flow. This proves that the membranes provide a good barrier against oxygen resulting in lower oxygen permeability across the membranes [92, 93].

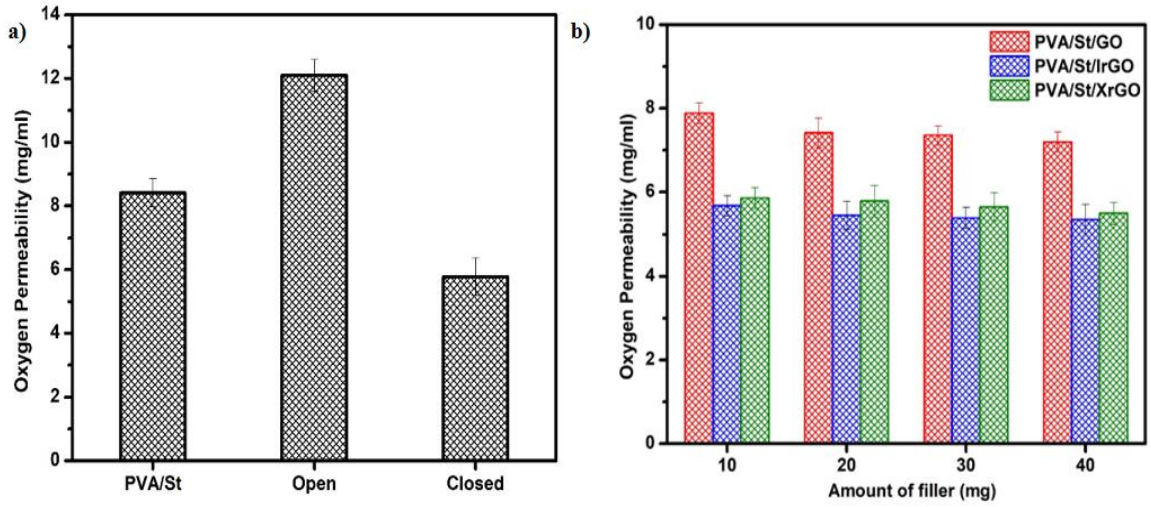

Figure 35 Oxygen permeability of membranes

4.9 Antibacterial Activity measurement:

The major purpose of food packaging is to safeguard food from being contaminated; main contributing factor for which is bacteria. The antibacterial activity in packaging films inhibits the bacterial growth on the food by providing direct contact of food surface with the film [94].

The antibacterial activity of PVA/St, PVA/St/GO, PVA/St/IrGO and PVA/St/XrGO membranes was inspected against two major food borne pathogens i.e. MRSA and E. Coli by using *"Agar Well Method"*[95]. As showm in Figure 36 and 37, the test revealed that PVA/St blank membrane, named as negative control, showed no antibacterial activity against both strains. Apart from PVA/St membranes all other membranes containing GO, IrGO and XrGO showed antibacterial exhibiting clear zone activity exhibiting clear zones PVA/St membranes all other membranes containing GO, IrGO and XrGO showed antibacterial activity exhibiting clear zones of inhibition.

Graphene oxide and GO containing materials show antibacterial activity against gram positive and gram negative bacteria [96-98]. Moreover, several researches were carried out to check the antibacterial activity of materials containing reduced graphene oxide and it was confirmed that rGO can be used as an effective antibacterial agent [96, 98, 99].

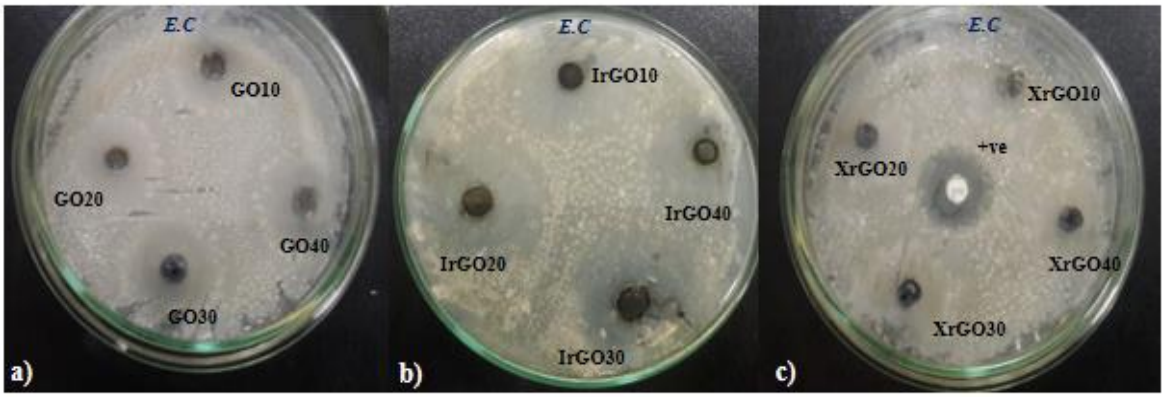

Figure 36 Antibacterial zones of inhibition against E. Coli

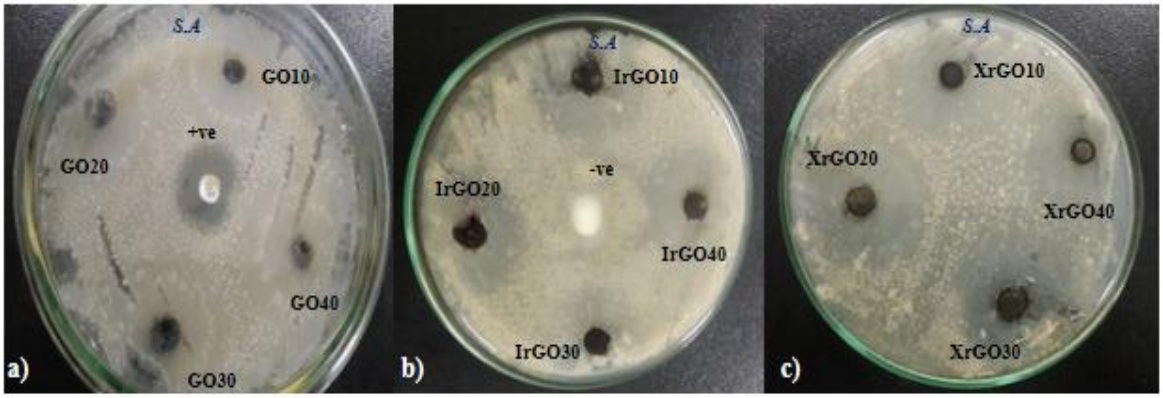

Figure 37 Antibacterial zones of inhibition against S. Aureus

The antibacterial activity of GO is widely attributed to different processes like oxidative stress, membrane stress, basal plane, photothermal effect and entrapment [99]. In addition, the blunt edges of GO's nanosheets can actually destroy bacterial membranes leading to intracellular matrix leakage causing bacterial inactivation [100, 101]. The antibacterial activity of rGO is dependent mainly on membrane stress and oxidative stress [99].

In this study, Vancomycin was used as a positive control which showed antibacterial activity against both bacterial strains; the diameter of zone of inhibition for E.Coli and S.Auerus was 25.67±0.5mm and 28.56±0.74mm respectively. In case of PVA/St/GO the maximum diameter of zone of inhibition was 30.46±0.45mm for E.Coli and 32.35±0.33mm for S.Auereus. For PVA/St/IrGO the maximum zone of inhibition for E.Coli and S.Auerus was 38.89±0.23mm and 37.52±0.41mm respectively. For PVA/St/XrGO the maximum dia of zone of inhibition was 35.66±0.63mm and 34.57±0.23mm for E.Coli and S.Auerus respectively.

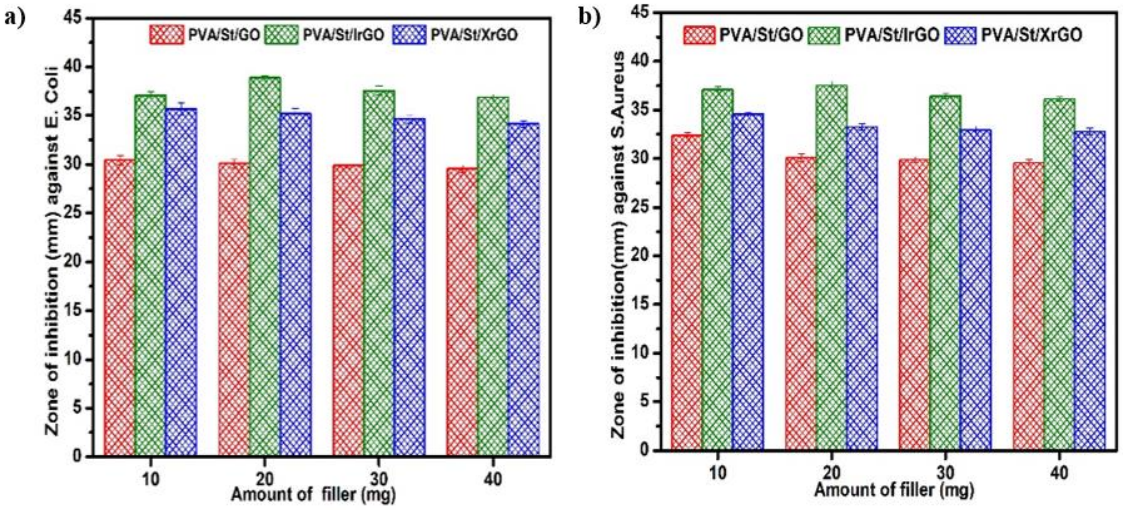

Figure 38 Zones of inhibition of membranes against a)E.Coli b)S.Aureus

4.10 Food packaging Test:

Among the synthesized membranes PVA/St, PVA/St/GO10, PVA/St/IrGO20 and PVA/St/XrGO10 were tested for food packaging. Phyllanthus emblica were washed, dried and packed in the aforementioned membranes also leaving one in open air as control. The packed samples and control were weighed each day and the percent weightloss was recorded every other day for 4 days.

The percent weight loss with time is shown in Figure 39. For open sample the percent weight loss was found to be 20.48% on day 4 while in the case of PVA/St the percent weight loss on day 4 was recorded as 12.78%. In case of PVA/St/GO10 membrane the percent weightloss was 9.98%. For PVA/St/IrGO20 overall least % weightloss was observed on day 4 showing that this provides an excellent barrier against moisture and oxygen permeability. Nearly comparable values were seen in the case of PVA/St/XrGO10.

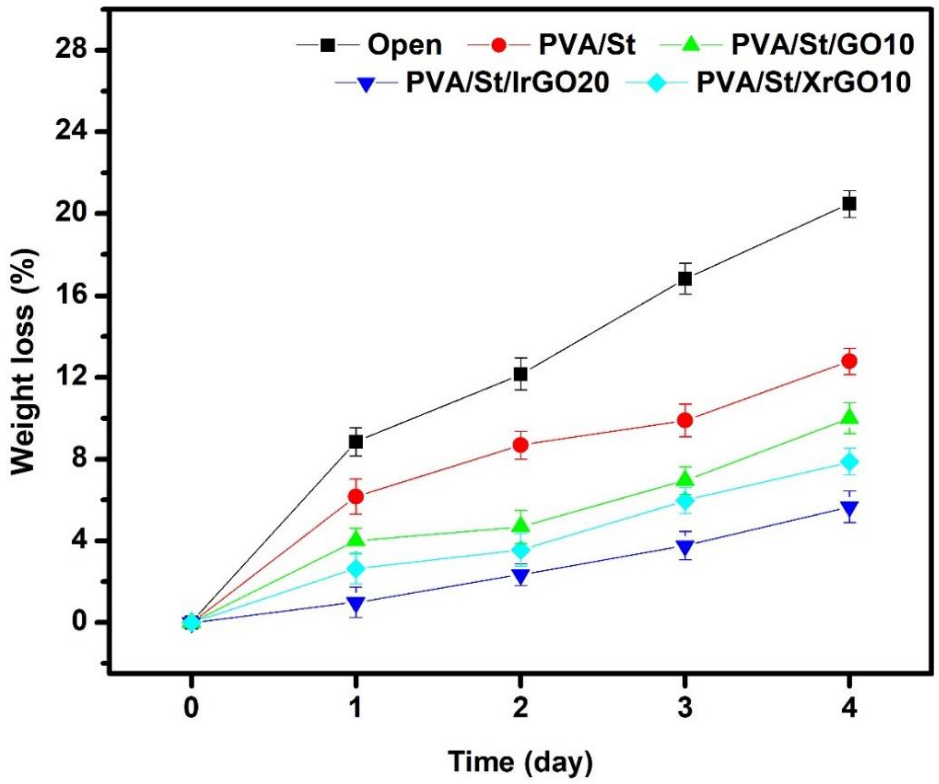

Figure 39 Percent weight loss versus time for Phyllanthus Emblica

The packed samples were opened after 4 days. The digital images of before and after 4 days are shown in Figure 40. It was observed that the control i.e. sample “a” was almost completely rotten. The fruit packed in PVA/St membrane, sample “b”, showed a larger rotten portion as it has no antibacterial activity. The fruit packed in PVA/St/GO, sample “c”, displayed very little scar showing putry. The fruit packed in PVA/St/IrGO and PVA/ST/XrGO, sample “d” and “e”, showed no visible changes on opening after 4 days of packing.

Figure 40 Images of packed fruit a) open b) PVA/St c) PVA/St/GO d) PVA/St/IrGO

The fruit in samples "c", "d" and "e" were further sliced to gain the insight of the interior of the fruit as shown in Figure 41. The fruit packed in PVA/St/GO showed very little decayed portion from the inside. The fruit in PVA/St/IrGO and PVA/St/XrGO showed no rotten portion from inside and the fruit appeared like as if it is freshly cut.

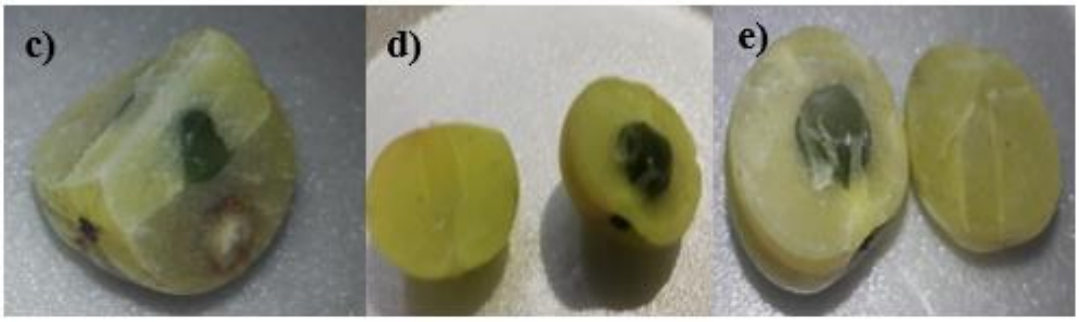

Figure 41 Image of sliced fruit c)PVA/St/GO d)PVA/St/IrGO e)PVA/St/XrGO

These results proved that PVA/St//IrGO is an excellent candidate to be used as food packaging membrane. Additionally, PVA/St/XrGO membrane gives almost similar kind of barrier properties.

4.11 Biodegradation Test:

The membranes PVA/St, PVA/St/GO10, PVA/St/IrGO20 and PVA/St/XrGO10 were cut in rectangular shape with dimensions 1x2 cm^2 represented in Figure 42 as a), b), c) and d) respectively. All membranes were weighed before burial and their pictures were clicked.

These were then folded in aluminium wire mesh and buried in rectangular box having dimension 10x5x6 cm^3 filled with soil. The soil was watered and the samples were taken out the next day. The pictures were taken which clearly showed that all samples degraded almost completely in soil. The % weight loss was found on the next day after burial as illustrated in Figure 43.

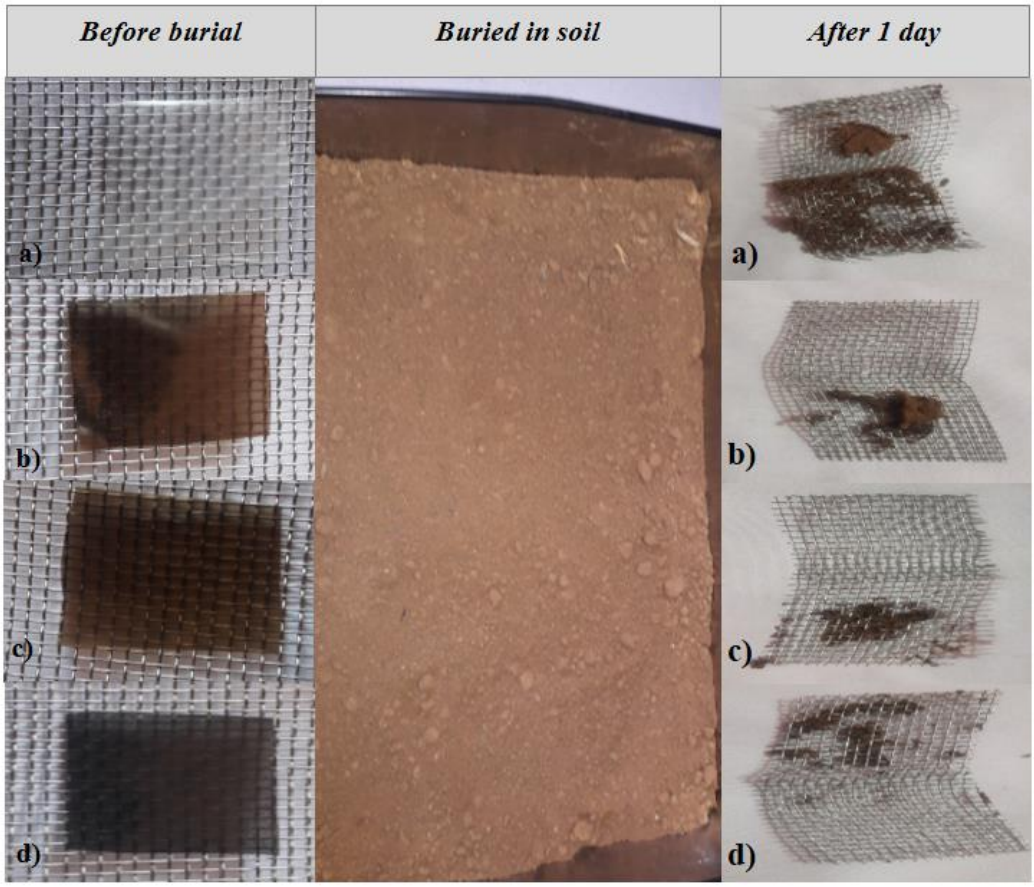

Figure 42 Pictorial representation of biodegradation of membranes a) PVA/St b) PVA/St/GO10 c) PVA/St/IrGO20 d) PVA/ST/XrGO10

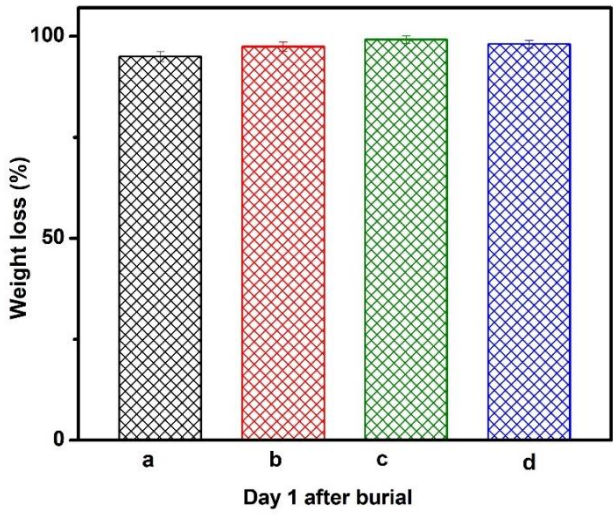

Figure 43 Percent Weightloss showing biodegradation

Conclusions:

Antibacterial films composed of PVA/Starch containing graphene oxide, insitu reduced graphene oxide and exsitu reduced graphene oxide were successfully synthesized. Among the synthesized membranes PVA/St/IrGO20 and PVA/St/XrGO20 showed remarkable mechanical properties. These membranes also provide an excellent barrier against water vapor and oxygen transmission rate. For PVA/St/IrGO the maximum zone of inhibition for E.Coli and S.Aureus was 38.89±0.23 mm and 37.52±0.41mm respectively. For PVA/St/XrGO the maximum dia of zone of inhibition was 35.66±0.63 mm and 34.57±0.23 mm for E.Coli and S.Aureus respectively. Thermal stability of PVA/St/IrGO membranes was found to be more as compared to other membranes. Food packaging test revealed that PVA/St/IrGO20 and PVA/St/XrGO10 remearkably increased the shelf life and preserved the freshness of Phylanthus Emblica. The soil burial test confirmed that the synthesized membranes were totally biodegradable.

Future recommendations:

Currently, people are learning about more about food safety. It is undeniable that there have been some controversies over the safety aspects of ready-made additives. Natural antimicrobial agents replace artificial additives. Scientists who develop antimicrobial films are carefully developing the use of natural compounds, such as plant extracts, as a substitute for use in antimicrobial foods. The perfect antimicrobial polymer foil should address some important factors, such as low processing cost. Secondly, the film must be chemically stable even after its prolonged use. Moreover, the antimicrobial film should act as a barrier against water and would not disintegrate easily, so that the antimicrobial effect remains unchanged. Also they should not be harmful to handle and should not release toxic particles into food.

References:

[1] A. Conte, L. Angiolillo, M. Mastromatteo, and M. A. Del Nobile, "Technological Options of Packaging to Control Food Quality," 2013.

[2] J. H. Han, "Chapter 1 - A Review of Food Packaging Technologies and Innovations," in *Innovations in Food Packaging (Second Edition)*, J. H. Han, Ed., ed San Diego: Academic Press, 2014, pp. 3-12.

[3] K. L. Yam, P. T. Takhistov, and J. Miltz, "Intelligent Packaging: Concepts and Applications," *Journal of Food Science*, vol. 70, pp. R1-R10, 2005/01/01 2005.

[4] F. Mohanty and S. K. Swain, "Bionanocomposites for Food Packaging Applications," pp. 363-379, 2017.

[5] A. K. Jassim, "Sustainable Solid Waste Recycling," 2017.

[6] M. Avella, J. J. De Vlieger, M. E. Errico, S. Fischer, P. Vacca, and M. G. Volpe, "Biodegradable starch/clay nanocomposite films for food packaging applications," *Food Chemistry*, vol. 93, pp. 467-474, 2005/12/01/ 2005.

[7] A. R. Rahman, K. S. Syamsu, and I. I. Isroi, "Biodegradability of Bioplastic in Natural Environment," *Jurnal Pengelolaan Sumberdaya Alam dan Lingkungan (Journal of Natural Resources and Environmental Management)*, vol. 9, pp. 258-263, 2019.

[8] J. Jayaramudu, G. S. M. Reddy, K. Varaprasad, E. R. Sadiku, S. Sinha Ray, and A. Varada Rajulu, "Preparation and properties of biodegradable films from Sterculia urens short fiber/cellulose green composites," *Carbohydrate Polymers*, vol. 93, pp. 622-627, 2013/04/02/ 2013.

[9] J. Rydz, M. Musioł, B. Zawidlak-Węgrzyńska, and W. Sikorska, "Present and Future of Biodegradable Polymers for Food Packaging Applications," pp. 431-467, 2018.

[10] K. L. Yam and D. S. Lee, "1 - Emerging food packaging technologies: an overview," in *Emerging Food Packaging Technologies*, K. L. Yam and D. S. Lee, Eds., ed: Woodhead Publishing, 2012, pp. 1-9.

[11] S. Yildirim, B. Röcker, M. K. Pettersen, J. Nilsen-Nygaard, Z. Ayhan, R. Rutkaite, *et al.*, "Active Packaging Applications for Food," *Comprehensive Reviews in Food Science and Food Safety*, vol. 17, pp. 165-199, 2018/01/01 2018.

[12] J.-W. Han, L. Ruiz-Garcia, J.-P. Qian, and X.-T. Yang, "Food Packaging: A Comprehensive Review and Future Trends," *Comprehensive Reviews in Food Science and Food Safety*, vol. 17, pp. 860-877, 2018.

[13] P. Prasad and A. Kochhar, "Active Packaging in Food Industry: A Review," *IOSR Journal of Environmental Science, Toxicology and Food Technology*, vol. 8, pp. 01-07, 01/01 2014.

[14] M. Sohail, D. W. Sun, and Z. Zhu, "Recent developments in intelligent packaging for enhancing food quality and safety," *Crit Rev Food Sci Nutr*, vol. 58, pp. 2650-2662, 2018.

[15] J.-D. Gu, "Microbiological deterioration and degradation of synthetic polymeric materials: recent research advances," *International Biodeterioration & Biodegradation*, vol. 52, pp. 69-91, 2003/09/01/ 2003.

[16] J. Rydz, W. Sikorska, M. Kyulavska, and D. Christova, "Polyester-based (bio)degradable polymers as environmentally friendly materials for sustainable development," *International journal of molecular sciences*, vol. 16, pp. 564-596, 2014.

[17] K. Khemani and C. Scholz, "Introduction and Overview of Degradable and Renewable Polymers and Materials," in *Degradable Polymers and Materials: Principles and Practice (2nd Edition)*. vol. 1114, ed: American Chemical Society, 2012, pp. 3-10.

[18] S. Sam, N. Mohd Amer, K. M. Chin, and N. Hani, "Current Application and Challenges on Packaging Industry Based on Natural Polymer Blending," ed, 2016, pp. 163-184.

[19] T. J. Madera-Santana, D. Robledo, and Y. Freile-Pelegrín, "Physicochemical Properties of Biodegradable Polyvinyl Alcohol–Agar Films from the Red Algae Hydropuntia cornea," *Marine Biotechnology*, vol. 13, pp. 793-800, 2011/08/01 2011.

[20] Z. W. Abdullah, Y. Dong, I. J. Davies, and S. Barbhuiya, "PVA, PVA Blends, and Their Nanocomposites for Biodegradable Packaging Application," *Polymer-Plastics Technology and Engineering,* vol. 56, pp. 1307-1344, 2017/08/13 2017.

[21] W. A. W. A. Rahman, L. Sin, A. Rahmat, and A. A. Samad, "Thermal behaviour and interactions of cassava starch filled with glycerol plasticized polyvinyl alcohol blends," *Carbohydrate Polymers,* vol. 81, pp. 805-810, 07/01 2010.

[22] M. Krumova, D. López, R. Benavente, C. Mijangos, and J. M. Pereña, "Effect of crosslinking on the mechanical and thermal properties of poly(vinyl alcohol)," *Polymer,* vol. 41, pp. 9265-9272, 12/01 2000.

[23] H.-R. Park, S.-H. Chough, Y.-H. Yun, and S.-D. Yoon, "Properties of Starch/PVA Blend Films Containing Citric Acid as Additive," *Journal of Polymers and the Environment,* vol. 13, pp. 375-382, 2005/10/01 2005.

[24] Y.-H. Yun, Y.-H. Na, and S.-D. Yoon, "Mechanical Properties with the Functional Group of Additives for Starch/PVA Blend Film," *Journal of Polymers and the Environment,* vol. 14, pp. 71-78, 01/01 2006.

[25] E. Karaoğul, e. altuntaş, T. Salan, and M. Hakki, "The Effects of Novel Additives Used in PVA/Starch Biohybrid Films," ed, 2018.

[26] A. Cano, M. Cháfer, A. Chiralt, and C. González-Martínez, "Physical and Antimicrobial Properties of Starch-PVA Blend Films as Affected by the Incorporation of Natural Antimicrobial Agents," *Foods (Basel, Switzerland),* vol. 5, p. 3, 2015.

[27] H. Ismail and N. F. Zaaba, "Effect of Additives on Properties of Polyvinyl Alcohol (PVA)/Tapioca Starch Biodegradable Films," *Polymer-Plastics Technology and Engineering,* vol. 50, pp. 1214-1219, 2011/08/01 2011.

[28] M. Roohani, Y. Habibi, N. Belgacem, G. Ebrahim, A. Karimi, and A. Dufresne, "Cellulose whiskers reinforced polyvinyl alcohol copolymers nanocomposites," *European Polymer Journal,* vol. 44, pp. 2489-2498, 08/01 2008.

[29] R. A. Talja, H. Helén, Y. H. Roos, and K. Jouppila, "Effect of various polyols and polyol contents on physical and mechanical properties of potato starch-based films," *Carbohydrate Polymers,* vol. 67, pp. 288-295, 2007/02/01/ 2007.

[30] O. A. Bin-Dahman, J. Jose, and M. A. Al-Harthi, "Effect of natural weather aging on the properties of poly(vinyl alcohol)/starch/graphene nanocomposite," *Starch - Stärke,* vol. 69, p. 1600005, 2017.

[31] S. Sali, H. R. Mackey, and A. A. Abdala, "Effect of Graphene Oxide Synthesis Method on Properties and Performance of Polysulfone-Graphene Oxide Mixed Matrix Membranes," *Nanomaterials (Basel),* vol. 9, May 19 2019.

[32] W. S. Hummers and R. E. Offeman, "Preparation of Graphitic Oxide," *Journal of the American Chemical Society,* vol. 80, pp. 1339-1339, 1958/03/01 1958.

[33] M. d. P. L. López, J. L. V. Palomino, M. L. S. Silva, and A. R. Izquierdo, "Optimization of the Synthesis Procedures of Graphene and Graphite Oxide," 2016.

[34] S. C. Ray, "Chapter 2 - Application and Uses of Graphene Oxide and Reduced Graphene Oxide," in *Applications of Graphene and Graphene-Oxide Based Nanomaterials*, S. C. Ray, Ed., ed Oxford: William Andrew Publishing, 2015, pp. 39-55.

[35] K. Tadyszak, J. Wychowaniec, and J. Litowczenko, "Biomedical Applications of Graphene-Based Structures," *Nanomaterials,* vol. 8, p. 944, 11/16 2018.

[36] K. K. H. De Silva, H. H. Huang, R. K. Joshi, and M. Yoshimura, "Chemical reduction of graphene oxide using green reductants," *Carbon,* vol. 119, pp. 190-199, 2017/08/01/ 2017.

[37] S. Stankovich, D. A. Dikin, R. D. Piner, K. A. Kohlhaas, A. Kleinhammes, Y. Jia, *et al.*, "Synthesis of graphene-based nanosheets via chemical reduction of exfoliated graphite oxide," *Carbon,* vol. 45, pp. 1558-1565, 2007/06/01/ 2007.

[38] A. Samal and D. Das, "Transfiguring UV light active “metal oxides” to visible light active photocatayst by reduced graphene oxide hypostatization," *Catalysis Today,* 03/27 2017.

[39] D. Ege, A. R. Kamali, and A. R. Boccaccini, "Graphene Oxide/Polymer-Based Biomaterials," *Advanced Engineering Materials,* vol. 19, p. 1700627, 2017.

[40] D. Liu, Q. Bian, Y. Li, Y. Wang, A. Xiang, and H. Tian, "Effect of oxidation degrees of graphene oxide on the structure and properties of poly (vinyl alcohol)

composite films," *Composites Science and Technology,* vol. 129, pp. 146-152, 2016/06/06/ 2016.

[41] X. An, H. Ma, B. Liu, and J. Wang, "Graphene Oxide Reinforced Polylactic Acid/Polyurethane Antibacterial Composites," *Journal of Nanomaterials,* vol. 2013, pp. 1-7, 2013.

[42] Y. Li, T. Yang, T. Yu, L. Zheng, and K. Liao, "Synergistic effect of hybrid carbon nantube–graphene oxide as a nanofiller in enhancing the mechanical properties of PVA composites," *Journal of Materials Chemistry,* vol. 21, pp. 10844-10851, 2011.

[43] X. Yang, S. Shang, and L. Li, "Layer-structured poly(vinyl alcohol)/graphene oxide nanocomposites with improved thermal and mechanical properties," *Journal of Applied Polymer Science,* vol. 120, pp. 1355-1360, 2011.

[44] X. Zhao, Q. Zhang, D. Chen, and P. Lu, "Enhanced Mechanical Properties of Graphene-Based Poly(vinyl alcohol) Composites," *Macromolecules,* vol. 43, pp. 2357-2363, 2010.

[45] C. Liu, J. Shen, K. W. K. Yeung, and S. C. Tjong, "Development and Antibacterial Performance of Novel Polylactic Acid-Graphene Oxide-Silver Nanoparticle Hybrid Nanocomposite Mats Prepared By Electrospinning," *ACS Biomaterials Science & Engineering,* vol. 3, pp. 471-486, 2017/03/13 2017.

[46] Y. Xu, W. Hong, H. Bai, C. Li, and G. Shi, "Strong and ductile poly(vinyl alcohol)/graphene oxide composite films with a layered structure," *Carbon,* vol. 47, pp. 3538-3543, 2009/12/01/ 2009.

[47] J. Ma, Y. Li, X. Yin, Y. Xu, J. Yue, J. Bao, *et al.*, "Poly(vinyl alcohol)/graphene oxide nanocomposites prepared by in situ polymerization with enhanced mechanical properties and water vapor barrier properties," *RSC Advances,* vol. 6, pp. 49448-49458, 2016.

[48] T. Cheng-an, Z. Hao, W. Fang, Z. Hui, Z. Xiaorong, and W. Jianfang, "Mechanical Properties of Graphene Oxide/Polyvinyl Alcohol Composite Film," *Polymers and Polymer Composites,* vol. 25, pp. 11-16, 2017/01/01 2017.

[49] Q. Chen, J. D. Mangadlao, J. Wallat, A. De Leon, J. K. Pokorski, and R. C. Advincula, "3D Printing Biocompatible Polyurethane/Poly(lactic acid)/Graphene

Oxide Nanocomposites: Anisotropic Properties," *ACS Applied Materials & Interfaces*, vol. 9, pp. 4015-4023, 2017/02/01 2017.

[50] C. Wang, Y. Li, G. Ding, X. Xie, and M. Jiang, "Preparation and characterization of graphene oxide/poly(vinyl alcohol) composite nanofibers via electrospinning," *Journal of Applied Polymer Science,* vol. 127, pp. 3026-3032, 2013.

[51] Y. Liu, M. Park, H. K. Shin, B. Pant, J. Choi, Y. W. Park, *et al.*, "Facile preparation and characterization of poly(vinyl alcohol)/chitosan/graphene oxide biocomposite nanofibers," *Journal of Industrial and Engineering Chemistry,* vol. 20, pp. 4415-4420, 2014/11/25/ 2014.

[52] R. Surudžić, A. Janković, M. Mitrić, I. Matić, Z. D. Juranić, L. Živković, *et al.*, "The effect of graphene loading on mechanical, thermal and biological properties of poly(vinyl alcohol)/graphene nanocomposites," *Journal of Industrial and Engineering Chemistry*, vol. 34, pp. 250-257, 2016.

[53] Y. Li, J. Sun, J. Wang, C. Qin, and L. Dai, "Preparation of well-dispersed reduced graphene oxide and its mechanical reinforcement in polyvinyl alcohol fibre," *Polymer International*, vol. 65, pp. 1054-1062, 2016.

[54] M. Gozutok, V. Sadhu, and H. T. Sasmazel, "Development of Poly(vinyl alcohol) (PVA)/Reduced Graphene Oxide (rGO) Electrospun Mats," *Journal of Nanoscience and Nanotechnology*, vol. 19, pp. 4292-4298, // 2019.

[55] S. Xie, B. Zhang, C. Wang, Z. Wang, L. Li, and J. Li, "Building up graphene-based conductive polymer composite thin films using reduced graphene oxide prepared by gamma-ray irradiation," *ScientificWorldJournal*, vol. 2013, p. 954324, 2013.

[56] D. C. Marcano, D. V. Kosynkin, J. M. Berlin, A. Sinitskii, Z. Sun, A. Slesarev, *et al.*, "Improved synthesis of graphene oxide," *ACS Nano,* vol. 4, pp. 4806-14, Aug 24 2010.

[57] S. N. Alam, N. Sharma, and L. Kumar, "Synthesis of Graphene Oxide (GO) by Modified Hummers Method and Its Thermal Reduction to Obtain Reduced Graphene Oxide (rGO)*," *Graphene,* vol. 06, pp. 1-18, 2017.

[58] N. Marturi, "Vision and visual servoing for nanomanipulation and nanocharacterization in scanning electron microscope," 11/19 2013.

[59] H. Agiwaan, "Thesis: Thermal Stability of cubic and nanocrystalline arc evaporated TiCrAlN coatings," 2014.

[60] M. Kot, "In-operando hard X-ray photoelectron spectroscopy study on the resistive switching physics of HfO2-based RRAM," 2014.

[61] D. Kumar, "Co-Functionalised Gold Nanoparticles for Drug Delivery Applications," 2012.

[62] N. P. Cheremisinoff, "2 - THERMAL ANALYSIS," in *Polymer Characterization*, N. P. Cheremisinoff, Ed., ed Westwood, NJ: William Andrew Publishing, 1996, pp. 17-24.

[63] Z. W. Abdullah, Y. Dong, N. Han, and S. Liu, "Water and gas barrier properties of polyvinyl alcohol (PVA)/starch (ST)/ glycerol (GL)/halloysite nanotube (HNT) bionanocomposite films: Experimental characterisation and modelling approach," *Composites Part B: Engineering,* vol. 174, p. 107033, 2019.

[64] S. S. Shojaeenezhad, M. Farbod, and I. Kazeminezhad, "Effects of initial graphite particle size and shape on oxidation time in graphene oxide prepared by Hummers' method," *Journal of Science: Advanced Materials and Devices,* vol. 2, pp. 470-475, 2017/12/01/ 2017.

[65] X. Jiao, Y. Qiu, L. Zhang, and X. Zhang, "Comparison of the characteristic properties of reduced graphene oxides synthesized from natural graphites with different graphitization degrees," *RSC Advances,* vol. 7, pp. 52337-52344, 2017.

[66] G. Wang, J. Yang, J. Park, X. Gou, B. Wang, H. Liu, *et al.*, "Facile Synthesis and Characterization of Graphene Nanosheets," *The Journal of Physical Chemistry C,* vol. 112, pp. 8192-8195, 2008/06/01 2008.

[67] L. Luo, T. Peng, M. Yuan, H. Sun, S. Dai, and L. Wang, "Preparation of Graphite Oxide Containing Different Oxygen-Containing Functional Groups and the Study of Ammonia Gas Sensitivity," *Sensors (Basel, Switzerland),* vol. 18, p. 3745, 2018.

[68] F. Tuz Johra, J. Lee, and W.-G. Jung, "Facile and safe graphene preparation on solution based platform," *Journal of Industrial and Engineering Chemistry,* vol. 20, pp. 2883–2887, 09/01 2014.

[69] V. Loryuenyong, K. Totepvimarn, P. Eimburanapravat, W. Boonchompoo, and A. Buasri, "Preparation and Characterization of Reduced Graphene Oxide Sheets via

Water-Based Exfoliation and Reduction Methods," *Advances in Materials Science and Engineering,* vol. 2013, p. 5, 2013.

[70] H. C. Schniepp, J.-L. Li, M. J. McAllister, H. Sai, M. Herrera-Alonso, D. H. Adamson, *et al.*, "Functionalized Single Graphene Sheets Derived from Splitting Graphite Oxide," *The Journal of Physical Chemistry B,* vol. 110, pp. 8535-8539, 2006/05/01 2006.

[71] A. Shalaby, D. Nihtianova, P. Markov, A. Staneva, R. Iordanova, and Y. Dimitriev, "Structural analysis of reduced graphene oxide by transmission electron microscopy," *Bulgarian Chemical Communications,* vol. 47, pp. 291-295, 01/01 2015.

[72] H. M. Kim, J. K. Lee, and H. S. Lee, "Transparent and high gas barrier films based on poly(vinyl alcohol)/graphene oxide composites," *Thin Solid Films,* vol. 519, pp. 7766-7771, 2011.

[73] H. K. Cheng, N. G. Sahoo, Y. P. Tan, Y. Pan, H. Bao, L. Li, *et al.*, "Poly(vinyl alcohol) nanocomposites filled with poly(vinyl alcohol)-grafted graphene oxide," *ACS Appl Mater Interfaces,* vol. 4, pp. 2387-94, May 2012.

[74] J. Ma, Y. Li, X. Yin, Y. Xu, J. Yue, J. Bao, *et al.*, "Poly(vinyl alcohol)/graphene oxide nanocomposites prepared by: In situ polymerization with enhanced mechanical properties and water vapor barrier properties," *RSC Adv.*, vol. 6, 05/18 2016.

[75] A. Rose, G. Prasad, T. Sakthivel, G. Venugopal, T. Maiyalagan, and T. V. Srm University, "Electrochemical Analysis of Graphene Oxide/Polyaniline/Polyvinyl Alcohol Composite Nanofibers for Supercapacitor Applications," *Applied Surface Science,* vol. 449, 03/01 2018.

[76] E. Abdel Bary, A. Fekri, and A. Harmal, "Aging of novel membranes made of PVA and cellulose nanocrystals extracted from Egyptian rice husk manufactured by compression moulding process," *International Journal of Environmental Studies,* vol. 75, pp. 750-762, 04/18 2018.

[77] B. K, V. Murugadoss, J. Lin, M. Dong, J.-x. Zhang, T. Li, *et al.*, "In situ grown nickel selenide on graphene nanohybrid electrodes for high energy density asymmetric supercapacitors," *Nanoscale,* vol. 10, 10/01 2018.

[78] A. Hassan, M. Niazi, A. Hussain, S. Farrukh, and T. Ahmad, "Development of Anti-bacterial PVA/Starch Based Hydrogel Membrane for Wound Dressing," *Journal of Polymers and the Environment*, 01/31 2017.

[79] A. Usman, Z. Hussain, A. Riaz, and A. N. Khan, "Enhanced mechanical, thermal and antimicrobial properties of poly(vinyl alcohol)/graphene oxide/starch/silver nanocomposites films," *Carbohydr Polym*, vol. 153, pp. 592-599, Nov 20 2016.

[80] J. Jose, M. A. Al-Harthi, M. A.-A. AlMa'adeed, J. Bhadra Dakua, and S. K. De, "Effect of graphene loading on thermomechanical properties of poly(vinyl alcohol)/starch blend," *Journal of Applied Polymer Science*, vol. 132, 2015.

[81] "<Jose_et_al-2015-Journal_of_Applied_Polymer_Science.pdf>."

[82] W. F. Wolkers, A. E. Oliver, F. Tablin, and J. H. Crowe, "A Fourier-transform infrared spectroscopy study of sugar glasses," *Carbohydrate Research*, vol. 339, pp. 1077-1085, 2004/04/28/ 2004.

[83] E. Sedaghat, A. A. Rostami, M. Ghaemy, and A. Rostami, "Characterization, thermal degradation kinetics, and morphological properties of a graphene oxide/poly (vinyl alcohol)/starch nanocomposite," *Journal of Thermal Analysis and Calorimetry*, vol. 136, pp. 759-769, 2018.

[84] S. Kashyap, S. K. Pratihar, and S. K. Behera, "Strong and ductile graphene oxide reinforced PVA nanocomposites," *Journal of Alloys and Compounds*, vol. 684, pp. 254-260, 2016/11/05/ 2016.

[85] M. S. Sarwar, M. Niazi, Z. Jahan, T. Ahmad, and A. Hussain, "Preparation and characterization of PVA/nanocellulose/Ag nanocomposite films for antimicrobial food packaging," *Carbohydrate Polymers*, vol. 184, 03/15 2018.

[86] K. Müller, E. Bugnicourt, M. Latorre, M. Jorda Beneyto, Y. Sanz, J. M. Lagaron, *et al.*, "Review on the Processing and Properties of Polymer Nanocomposites and Nanocoatings and Their Applications in the Packaging, Automotive and Solar Energy Fields," *Nanomaterials*, vol. 7, p. 47, 04/07 2017.

[87] V. Loryuenyong, C. Saewong, C. Aranchaiya, and A. Buasri, "The Improvement in Mechanical and Barrier Properties of Poly(Vinyl Alcohol)/Graphene Oxide Packaging Films," *Packaging Technology and Science*, vol. 28, pp. 939-947, 2015.

[88] M. Tolinski, "Gas Barrier Properties Enhancement," pp. 171-173, 2015.

[89] L. W. Winkler, "Die Bestimmung des im Wasser gelösten Sauerstoffes," *Berichte der deutschen chemischen Gesellschaft,* vol. 21, pp. 2843-2854, 1888/07/01 1888.

[90] G. Lu, K. Ling, P. Zhao, Z. Xu, C. Deng, H. Zheng, *et al.*, "A novel in situ-formed hydrogel wound dressing by the photocross-linking of a chitosan derivative," *Wound Repair Regen,* vol. 18, pp. 70-9, Jan-Feb 2010.

[91] D. Zhang, W. Zhou, B. Wei, X. Wang, R. Tang, J. Nie, *et al.*, "Carboxyl-modified poly(vinyl alcohol)-crosslinked chitosan hydrogel films for potential wound dressing," *Carbohydr Polym,* vol. 125, pp. 189-99, Jul 10 2015.

[92] S. Wittaya-areekul and C. Prahsarn, "Development and in vitro evaluation of chitosan-polysaccharides composite wound dressings," *Int J Pharm,* vol. 313, pp. 123-8, Apr 26 2006.

[93] B. Singh and L. Pal, "Sterculia crosslinked PVA and PVA-poly(AAm) hydrogel wound dressings for slow drug delivery: mechanical, mucoadhesive, biocompatible and permeability properties," *J Mech Behav Biomed Mater,* vol. 9, pp. 9-21, May 2012.

[94] B. Malhotra, A. Keshwani, and H. Kharkwal, "Antimicrobial food packaging: potential and pitfalls," *Frontiers in microbiology,* vol. 6, pp. 611-611, 2015.

[95] U. Bagul and S. Sivakumar, "Antibiotic Suspectibility Testing: A Review on Current Practices," *International Journal of Pharmacy,* vol. 6, pp. 11-17, 01/01 2016.

[96] S. Szunerits and R. Boukherroub, "Antibacterial activity of graphene-based materials," *Journal of Materials Chemistry B,* vol. 4, pp. 6892-6912, 2016.

[97] O. Akhavan and E. Ghaderi, "Toxicity of Graphene and Graphene Oxide Nanowalls Against Bacteria," *ACS Nano,* vol. 4, pp. 5731-5736, 2010/10/26 2010.

[98] I. Sengupta, P. Bhattacharya, M. Talukdar, S. Neogi, S. K. Pal, and S. Chakraborty, "Bactericidal effect of graphene oxide and reduced graphene oxide: Influence of shape of bacteria," *Colloid and Interface Science Communications,* vol. 28, pp. 60-68, 2019/01/01/ 2019.

[99] P. Kumar, P. Huo, R. Zhang, and B. Liu, "Antibacterial Properties of Graphene-Based Nanomaterials," *Nanomaterials (Basel),* vol. 9, May 13 2019.

[100] S. Liu, T. H. Zeng, M. Hofmann, E. Burcombe, J. Wei, R. Jiang, *et al.*, "Antibacterial Activity of Graphite, Graphite Oxide, Graphene Oxide, and Reduced Graphene Oxide: Membrane and Oxidative Stress," *ACS Nano*, vol. 5, pp. 6971-6980, 2011/09/27 2011.

[101] X. Li, F. Li, Z. Gao, and L. Fang, "Toxicology of Graphene Oxide Nanosheets Against Paecilomyces catenlannulatus," *Bulletin of environmental contamination and toxicology*, vol. 95, 03/20 2015.